MISCELLANEOUS PAPER GL-84-8

PROBABILISTIC ROCK SLOPE ENGINEERING

by

Stanley M. Miller

Geotechnical Engineer
509 E. Calle Avenue
Tucson, Arizona 85705

June 1984
Final Report

Prepared for DEPARTMENT OF THE ARMY
US Army Corps of Engineers
Washington, DC 20314

Under CWIS Work Unit 31755

Monitored by Geotechnical Laboratory
US Army Engineer Waterways Experiment Station
PO Box 631, Vicksburg, Mississippi 39180

my Corps
gineers

GEOTECHNICAL LABORATORY

Unclassified

SECURITY CLASSIFICATION OF THIS PAGE *(When Data Entered)*

REPORT DOCUMENTATION PAGE

READ INSTRUCTIONS BEFORE COMPLETING FORM

1. REPORT NUMBER
Miscellaneous Paper GL-84-8

2. GOVT ACCESSION NO.

3. RECIPIENT'S CATALOG NUMBER

4. TITLE *(and Subtitle)*
PROBABILISTIC ROCK SLOPE ENGINEERING

5. TYPE OF REPORT & PERIOD COVERED
Final report

6. PERFORMING ORG. REPORT NUMBER

7. AUTHOR(s)
Stanley M. Miller

8. CONTRACT OR GRANT NUMBER(s)

9. PERFORMING ORGANIZATION NAME AND ADDRESS
Stanley M. Miller
Geological Engineer
509 E. Calle Avenue, Tucson, Arizona 85705

10. PROGRAM ELEMENT, PROJECT, TASK AREA & WORK UNIT NUMBERS
CWIS Work Unit 31755

11. CONTROLLING OFFICE NAME AND ADDRESS
DEPARTMENT OF THE ARMY
US Army Corps of Engineers
Washington, DC 20314

12. REPORT DATE
June 1984

13. NUMBER OF PAGES
75

14. MONITORING AGENCY NAME & ADDRESS*(If different from Controlling Office)*
US Army Engineer Waterways Experiment Station
Geotechnical Laboratory
PO Box 631, Vicksburg, Mississippi 39180

15. SECURITY CLASS. *(of this report)*
Unclassified

15a. DECLASSIFICATION/DOWNGRADING SCHEDULE

16. DISTRIBUTION STATEMENT *(of this Report)*
Approved for public release; distribution unlimited.

17. DISTRIBUTION STATEMENT *(of the abstract entered in Block 20, if different from Report)*

18. SUPPLEMENTARY NOTES
Available from National Technical Information Service, 5285 Port Royal Road, Springfield, Virginia 22161.

19. KEY WORDS *(Continue on reverse side if necessary and identify by block number)*
Rock slopes--Stability (LC)
Probabilities (LC)
Slopes (Physical geography) (LC)
Geology, Structural (LC)
Engineering--Statistical methods (LC)

20. ABSTRACT *(Continue on reverse side if necessary and identify by block number)*
Natural variabilities in rock mass properties and uncertainties in their measurement and estimation imply the probabilistic nature of parameters required for rock slope engineering. Therefore, statistical and probabilistic methods are important for studying mapped fracture data, analyzing rock strength testing data, and evaluating rock slope stability. Such methods provide a realistic treatment of parameter variabilities and lead to probabilistic slope design criteria.

(Continued)

DD FORM 1 JAN 73 1473 EDITION OF 1 NOV 65 IS OBSOLETE

Unclassified

SECURITY CLASSIFICATION OF THIS PAGE *(When Data Entered)*

20. ABSTRACT (Continued).

Rock slope engineering requires information about geologic structures because slope failures in rock masses commonly occur along structural discontinuities. Stability of rock slopes is primarily governed by the geometric properties and shear strengths of geologic discontinuities and also by the local stress field. Natural variabilities in these rock mass properties and uncertainties in their measurement and estimation imply the probabilistic nature of input parameters needed for rock slope engineering.

In a probabilistic slope stability analysis the input parameters are considered as random variables that must be statistically described. The descriptive process relies on statistical analyses of discontinuity data collected by field mapping and of laboratory and field test results. Sound geologic and engineering judgement should be used in conjunction with these analyses.

The probability of stability for a given slope failure mode is estimated by combining the probability of sliding and the probability that the potential sliding surface is long enough to allow failure. The probability of sliding is calculated from a safety factor distribution which can be estimated by Monte Carlo simulation or by numerical convolution performed by discrete Fourier procedures. The probability of sifficient length is estimated from discontinuity length data obtained by structure mapping.

Multiple occurrences of the same failure mode in a slope can be analyzed after they have been simulated by generating spatially correlated properties of discontinuities responsible for the failure mode. A probabilistic analysis also allows for the effects of different failure modes in the same slope to be combined into a probabilistic estimate of overall slope stability. Thus, rock slope engineering can be enhanced by probabilistic methods that allow for a realistic treatment of parameter variabilities and multiple failure modes and that also produce useful probabilistic slope design criteria.

PREFACE

This report was written by Dr. Stanley M. Miller for the U. S. Army Engineer Waterways Experiment Station (WES), Vicksburg, Mississippi. Dr. Miller is presently a professor in the Department of Geology at Washington State University. The report was sponsored by the Office, Chief of Engineers (OCE), U. S. Army, under the Civil Works Investigational Studies (CWIS), Rock Research Program (Work Unit 31755) on "Probabilistic Methods in Engineering Geology." OCE technical monitor was Mr. Paul R. Fisher. At WES, the work was under the management of the Earthquake Engineering and Geophysics Division (EEGD), Geotechnical Laboratory (GL). The GL technical monitor was Ms. Mary Ellen Hynes-Griffin, EEGD. Dr. Arley G. Franklin was Chief, EEGD, and Dr. William F. Marcuson III was Chief, GL, during the preparation of this report.

Portions of this report represent partial results of Ph.D. research conducted by the author in 1981 and 1982 at the University of Wyoming and funded by Climax Molybdenum Company, a subsidiary of AMAX, Inc., of Golden, Colo.

COL Tilford C. Creel, CE, was Commander and Director of WES during the preparation of this report. Mr. Fred R. Brown was Technical Director.

CONTENTS

PROBABILISTIC ROCK SLOPE ENGINEERING

PART I: INTRODUCTION

1. The engineering design of slopes cut in discontinuous rock requires information about geologic structures because slope failures commonly occur along structural discontinuities. For this reason, rock slope engineering demands a different approach than the engineering of soil or soft-rock slopes in which failures follow circular-type surfaces of minimum strength through the material substance. Intensely fractured or highly weathered rock materials usually are also included in the soil slope category.

Factors Influencing Rock Slope Stability

2. Slope stability in rock masses is primarily governed by the geometric characteristics and the shear strengths of geologic discontinuities and by the local stress field. Important geometric characteristics are the orientation (dip and dip direction), spacing, length or extent, and waviness (difference between average dip and minimum dip). The shear strength along a discontinuity depends on its physical character, which includes its thickness, type of filling material, type of wall rock, and surface roughness due to asperities. The stress field acting in a slope is controlled by the unit weight of the rock, ground-water pressures, and possibly tectonic stresses and other stresses due to the local geologic history.

3. Natural variabilities in these rock mass properties and measurement uncertainties associated with their estimation imply the probabilistic nature of the input parameters needed for rock slope engineering. A deterministic slope design based on the average values of input parameters does not take into account statistical variabilities and may provide misleading results. In fact, some deterministic geotechnical analyses can lead to a supposedly conservative design that actually has a substantial probability of failure (Hoeg and Murarka 1974).

4. A probabilistic slope stability analysis can only be conducted if the input parameters are considered as random variables and have been statistically quantified and described. This descriptive process relies on the collection and analysis of field data, the results of laboratory and field tests,

and on geologic and engineering judgment. Probability distributions of fracture* characteristics can be estimated from field mapping data usually obtained by either surface fracture mapping or oriented core logging or both. Shear strengths along fractures can be estimated by statistically analyzing the results of laboratory direct shear tests of rock specimens that contain natural fractures. Laboratory tests can also be used to estimate the unit weight of the rock. Ground-water pressures acting in the slope are usually predicted by hydrologic field tests and measurements. If a slope design project warrants the additional effort and expense, then a field rock mechanics study can be conducted to measure local tectonic and residual stresses or an earthquake study used to evaluate potential site displacements and accelerations.

The Emergence of Probabilistic Slope Engineering

5. Probabilistic methods in rock slope engineering have been developed during the last 15 years or so and have their roots and support in the mining industry. Current economic evaluations of open pit mines are often based on the application of sophisticated statistical or simulation methods that require input from probabilistic slope stability analyses (Kim and Wolff 1978). Such analyses are essential because slope angles have a significant economic impact on any open pit mining operation.

6. Economic simulation of an open pit mine requires that the probabilities of failure be specified for various slope heights and angles in all sectors of the pit. These probability values are calculated or estimated by analyzing all potential failure modes at several incremental slope heights and angles. Then, for each pit sector the results are compiled in a table, usually called the probability of failure schedule, for that sector. A set of these schedules is needed for a cost-benefit analysis in which the mine life is simulated at incremental time periods.

7. During the simulation, a slope failure is considered to occur if a generated, uniform random number is less than the probability of failure value for the specified slope geometry. Cost of the failure is estimated from mine

---

* The term "fracture" will be used interchangeably with the term "discontinuity" because the most common geologic discontinuities in rock are fractures, which are either joints (along which there has been no displacement) or faults (along which there has been displacement).

planning and operational forecasts. An accounting is made for all mining costs and benefits incurred during each time period and the overall results compiled at the end of the simulated mine life. By conducting the simulation for several overall pit slope angles, a plot relating slope angle and net profit can be constructed and then used to select the economically optimum slope angle. Results from such a study provide valuable information for corporate decision makers, particularly in the case of economically marginal mineral deposits.

8. Probabilistic slope engineering methods are also applicable to civil works projects, such as the design of road cuts or other man-made slopes in fractured rock masses. However, the usage of probabilistic tools by civil engineers has been hampered by differences in design philosophy, the major contrast being that risk levels acceptable for mining projects are not acceptable for most civil projects. Mining ventures can usually tolerate higher risks because of relatively short mine lives, the desire to maximize profit, and the implementation of slope monitoring programs to provide safe working conditions. Regardless of the differences between mining and civil design approaches, the basic statistical, geological, and engineering tools are the same for quantifying probabilities of slope failure. Such quantification is becoming more and more relevant for civil works projects with the major benefit being a realistic treatment and incorporation of natural variabilities and measurement uncertainties.

Overview of Probabilistic Slope Engineering Procedures

9. Any rock slope engineering project should begin with a thorough evaluation of regional and local geology. After major rock units and structural features have been identified, spot mapping techniques are used in the study area to collect detailed information about fracture characteristics and about other structural features if they are present. The sampled fracture orientations obtained at each mapping site can then be displayed on lower-hemisphere Schmidt plots. Visual comparisons or statistical evaluations of the plots allow for the identification of structural domain boundaries. A structural domain represents an area characterized by a distinct rock unit or by a distinct pattern of fracture orientations.

10. Potential orientations of the slope cut and the locations of

structural domains are used together to select design sectors, each of which has a distinct slope face strike in a given structural domain. Kinematically viable slope failure modes are then identified in each sector by evaluating how the fracture orientations mapped in the particular structural domain interact with the slope face orientation. Lower-hemisphere Schmidt plots that display poles to fractures are usually considered essential in this process of predicting potential failure modes (Hoek and Bray 1977).

11. Fracture sets that cause potential failure modes are often called design sets because they tend to be critical to the slope design. The original fracture mapping data are used to construct histograms and to estimate the probability distributions of pertinent characteristics in the design sets. Typically, the dip and dip direction in a design set are normally distributed and the spacing, length, and waviness are exponentially distributed.

12. Shear strengths along fractures in the design sets can be estimated by laboratory direct shear tests of rock specimens that contain natural fractures. Each specimen should be oriented in situ and so marked prior to removal from the outcrop or drill core; this allows for the testing shear direction to coincide with the natural down-dip direction of the fracture. Test results are presented as a plot of shear strength as a function of normal stress. Least-squares regression procedures are then applied to the data to estimate the mean and variance of the shear strength at any given normal stress.

13. Laboratory tests of rock samples are commonly used to measure the rock unit weight, which tends to be normally distributed. Hydrologic field tests (such as pump tests and drawdown tests) are used to estimate permeabilities, and measurements of water levels in drill holes provide a means of estimating ground-water levels in the study area. Procedures for converting this hydrologic information to a probability distribution of water pressures in the slope are somewhat limited at the present time and usually rely on simulation methods (Miller 1982a).

14. After all of the above input parameters have been statistically described, probabilistic stability analyses can be conducted for the failure modes identified in each design sector. The probability of sliding for any common failure mode can be estimated by either of two methods. Monte Carlo simulation relies on repeated sampling of input values from the given probability distributions to calculate a number of possible safety factors. The

probability of sliding is defined as the area under the safety factor distribution where values are less than one or as the simple percentage of simulated safety factors that are less than one. The other method consists of directly determining the safety factor distribution by convolution of the probability distributions of the proper input variables.

15. The probability of failure for a given failure mode equals the product of the following: probability of sliding, probability of daylighting (i.e., sliding path dips flatter than the slope face), and probability that the sliding surface is long enough to allow failure. The latter two probabilities are usually calculated directly by using the respective dip and length distributions and the proposed slope geometry.

16. Applications of finite element and finite difference methods to rock slope stability analyses have not been especially effective or successful to date, mainly due to the inhomogeneous nature of discontinuous rock and the difficulty in incorporating the statistical variability of fracture properties. The methods can be useful when simplifying assumptions are made and when the specific locations and properties of potential failure surfaces are known, but even then the associated conputational costs are usually too great to justify the final results.

PART II: MAPPING AND DISPLAY OF FRACTURE DATA

17. Dominant geologic structures such as major faults and lithologic contacts are usually considered individually in rock slope engineering projects because they occur in definable locations and are continuous over distances comparable to the size of the study area. In contrast, structures such as fractures and foliations have high frequencies of occurrence and are discontinuous over the study area. They are too numerous to be mapped individually and, therefore, should be considered in a statistical manner.

Rationale of Fracture Mapping

18. Geometric characteristics of fractures, including orientation, spacing, length, and waviness, are random variables that can be modeled by statistical distributions estimated from mapping data (Call, Savely, and Nicholas 1976). Necessary fracture data can be collected by surface mapping techniques (Piteau 1970, Call 1972, and McMahon 1974) and by oriented-core logging. To map in detail every exposed fracture within a given area is impractical, if not impossible. Therefore, spot mapping is relied upon to provide a sample or samples of the fracture population from which distributions of the fracture properties can be estimated.

19. After a geologic mapping and evaluation program has been completed for the study area, a geologic map should be constructed to emphasize the rock units present, their contacts, and any major structures that may affect the stability of the proposed slope. This map, in conjunction with field knowledge of the area, provides the major basis for designing a fracture mapping program. At least one or two mapping sites are desired within each anticipated structural domain, and these sites should be located so as to help delineate and further define the domains. Careful thought and planning of the mapping program cannot be overemphasized, because much time and money has been wasted by field sampling that has not been properly planned and directed.

20. If possible, the mapping samples should be random and representative so as not to make the population estimates biased or unrealistically weighted. Such samples are often difficult to obtain in the study area because surface outcrop exposures are usually limited and biased toward the more competent rock materials. This sampling problem can be offset somewhat by

mapping man-made cuts along construction or development roads and by oriented-core logging of drill holes, even though such sites may be located for purposes other than for fracture mapping and may have physical access limitations. Therefore, the slope engineer must remember that the interpretive step in estimating population parameters from sample data should be guided by subject-matter knowledge, experience, and judgment (see Whitten 1966).

Examples of Mapping Techniques

21. Many fracture mapping techniques are currently in use for collecting fracture data pertinent to rock engineering projects. The selection of mapping methods and styles primarily depends on the mapper's personal preference, the site geology, the size of the project, the availability of mappable exposures, and the time and manpower allocated for the mapping task. However, most mapping schemes are variations of three fundamental techniques, fracture-set mapping (or cell mapping), detail-line mapping, and oriented-core logging. Examples of these techniques that have been used extensively in rock engineering practice during recent years are described below. Suggested mapping forms (e.g., field data sheets) that allow for rapid computer processing are also presented, but it should be remembered that variations or modifications may be required for individual mapping programs.

Fracture-set mapping

22. Fracture-set mapping, which is also known as cell mapping, is a systematic method for gathering information about fracture sets and for helping to delineate structural domains. This mapping method is particularly valuable in situations where fracture data must be collected over a large area in a short time period. It also provides information useful for evaluating variations in fracture patterns over the study area.

23. Natural outcrops and man-made exposures are located and identified as potential mapping sites. Long or extensive rock exposures are divided into mapping cells of a regular, manageable size, usually about 8 to 12 m in length. In each mapping cell the dominant four or five fracture sets are recognized by locating groups of two or more approximately parallel fractures. Exceptionally large single joints and faults are also located, which will be mapped as individuals. Measurements of geometric characteristics and other information are then recorded for each fracture set or major structure in the cell.

24. An example of a field data sheet for recording fracture-set mapping data is shown in Figure 1. Required basic information includes the project

DATA SHEET FOR STRUCTURE MAPPING

PAGE ____ OF ____

BY _____

IDENT NO. ☐☐☐☐☐☐☐☐ LOCATION _____ DATE _____

COORDINATES NORTH	COORDINATES EAST	ROCK TYPE A	ROCK TYPE B	STRUCTURE TYPE	STRUCTURE STK	STRUCTURE DIP	GEOMETRY MD	GEOMETRY LENGTH	GEOMETRY SPACING DIST.	GEOMETRY SPACING NO.	GEOMETRY T_1	GEOMETRY T_2	GEOMETRY R	THICK-NESS( )	FILLING N	FILLING W	CL. NO.

ROCK TYPE ABBREVIATIONS			

STRUCTURE TYPE ABBREVIATIONS			
SJ	SINGLE JOINT		
FT	FAULT		
CT	CONTACT		
TERMINATIONS			
H	>20°	R	IN ROCK
L	<20°	N	NONE
		E	EN ECHELON

FILLING ABBREVIATIONS				N	NONE
WATER D=DRY W=WET F=FLOWING S=SQUIRTING					
R=ROUGHNESS S,R					
MD=MINIMUM DIP					

Figure 1. Example of data recording sheet for fracture-set mapping (from the Rock Mechanics Division of Pincock, Allen, Holt, Inc., Tucson, Ariz.)

location, mapper's name, date, and an identification number for the particular area being mapped. At a given mapping cell, or site, the following information is recorded on the illustrated data sheet for each fracture set or major structure:

a. Coordinates. The approximate map coordinates of the cell are recorded after being determined by map inspection, compass and pace techniques, or surveying. These coordinates are repeated for each fracture set or major structure observed in the mapping cell.

b. Rock type. The rock type (or types) in which the mapping is being conducted is recorded using a three-letter alpha code.

c. Structure type. A two-letter alpha code is used to identify the type of structural feature being described. The most common code is "JS" for joint set.

d. Structure orientation. The overall average dip and azimuth strike of the fracture set are recorded using a right-hand convention whereby the dip direction is 90 deg clockwise from the strike direction; this defines the orientation by a two-number designation.

e. Minimum dip (MD). The dip of the flattest fracture in the set is noted. For a single major structure the minimum dip is the dip of the flattest portion of its surface.

f. Length. The maximum traceable distance of the longest fracture in the set (or of the single major structure) is recorded; this length is often limited by outcrop dimensions.

g. Spacing. The number of fractures in the set and the distance between the outer two, as measured normal to the fractures, are recorded to provide data for calculating the mean fracture spacing. These measurements are not applicable to single major structures.

h. Terminations, roughness, thickness, filling, and water (W). These data are recorded only for individual major structures. Descriptions of these measurements or observations are given later in this Part.

25. In a study area with accessible rock exposures an experienced mapper can typically map a dozen or more cells per day. If possible, at least five or six cells should be mapped in each rock unit or suspected structural domain. In remote areas with little or no construction and development the mapping program should attempt to include most outcrops large enough to be mapped. By comparing fracture-set data (especially the orientations) from different mapping cells the boundaries of structural domains may be better defined. Another major benefit derived from a thorough fracture-set mapping program is that specific sites for collecting more detailed fracture information can be identified.

Detail-line mapping

26. Detail-line mapping is a systematic spot sampling technique for obtaining detailed information about the geometric characteristics of fractures and other geologic structural features. A measuring tape is stretched across the outcrop or exposure to be mapped. Using the tape as a reference line, a mapping zone (e.g., sampling area) is defined that extends 1 m above and 1 m below the line. The length of the mapping zone, or window, is determined by

the complexity of the structural pattern and, accordingly, this length serves as a measure of fracture intensity. All structural features that occur at least partially in the zone are mapped, though a minimum length cutoff of 10 cm is typically enforced. That is, features with trace lengths less than this cutoff are not mapped. Experience has shown that a minimum of approximately 150 fracture observations per line is desirable for statistical evaluations (Call, Savely, and Nicholas 1976).

27. An example of a field data sheet for recording detail-line mapping data is shown in Figure 2. Basic information recorded for each mapping site includes the line identification number, location, date, mapper's name, bearing and plunge of the measuring tape, and attitude (orientation) of the rock exposure.

DATA SHEET FOR DETAIL-LINE MAPPING

PAGE___ OF___

BEARING PLUNGE STRIKE DIP LINE NO. ELEV._____ LOCATION _____ BY_____ DATE_____

DIST. ( )	ROCK TYPE A	ROCK TYPE B	STRUCTURE TYPE	STRUCTURE STK	STRUCTURE DIP	GEOMETRY MD	GEOMETRY P	GEOMETRY LENGTH	GEOMETRY ± OVERLAP	GEOMETRY T_1	GEOMETRY T_2	GEOMETRY R	THICK-NESS( )	FILLING N	W	CL. NO.

ROCK TYPE ABBREVIATIONS

STRUCTURE TYPE

SJ	SINGLE JOINT
FT	FAULT
CT	CONTACT

GEOMETRY

P=PL// R=ROUGHNESS-S,R,M

MD=MINIMUM DIP

TERMINATION

H	>20°	R	IN ROCK
L	<20°	N	NONE
		E	EN ECHELON

WATER D=DRY W=WET F=FLOWING S=SQUIRTING

FILLING ABBREVIATIONS

N	NONE

OVERLAP

MEASURED FROM TAPE ALONG TRACE OR PROJECTED TRACE TO BOTTOM OF JOINT

+ ABOVE TAPE, - BELOW TAPE

Figure 2. Example of data recording sheet for detail-line mapping (from the Rock Mechanics Division of Pincock, Allen, and Holt, Inc., Tucson, Ariz.)

28. For each discontinuity occurring within the mapping zone the following information is recorded on the illustrated data sheet:

a. Distance. This is the distance along the measuring tape where the fracture or its projection intersects the tape. For any fracture parallel to the tape the distance at the middle of the fracture trace is recorded.

b. Rock type. The rock type (or types) in which the fracture occurs is recorded by using a three-letter alpha code.

c. Structure type. A two-letter alpha code is used to identify the type of discontinuity being described.

d. Structure orientation. Average dip and azimuth strike of the fracture are recorded using a right-hand convention whereby the dip direction is 90 deg clockwise from the strike direction; this defines the fracture orientation by a two-number designation.

e. Minimum dip (MD). Dip on the flattest portion of the fracture surface is recorded to compare with the average dip. Their difference serves as a quantitative measure of the fracture waviness.

f. Parallel (P). A fracture parallel to the measuring tape is so designated by a letter "P" in this column.

g. Length. Fracture length is the maximum traceable distance observed, which often extends beyond the mapping zone and is limited by outcrop dimensions. Lengths should be measured with a hand-held tape, but longer fracture lengths (greater than approximately 10 ft) may have to be estimated.

h. Overlap. Overlap is the distance one fracture extends over the next fracture of the same set. For field mapping the measurement is usually made along the trace length of each fracture and equals the distance from the bottom termination to the mapping tape (Figure 3). If the fracture terminates below the tape, a minus distance is recorded. The true overlap can then be calculated later from the field measurements. Overlap is not applicable for fractures parallel to the tape.

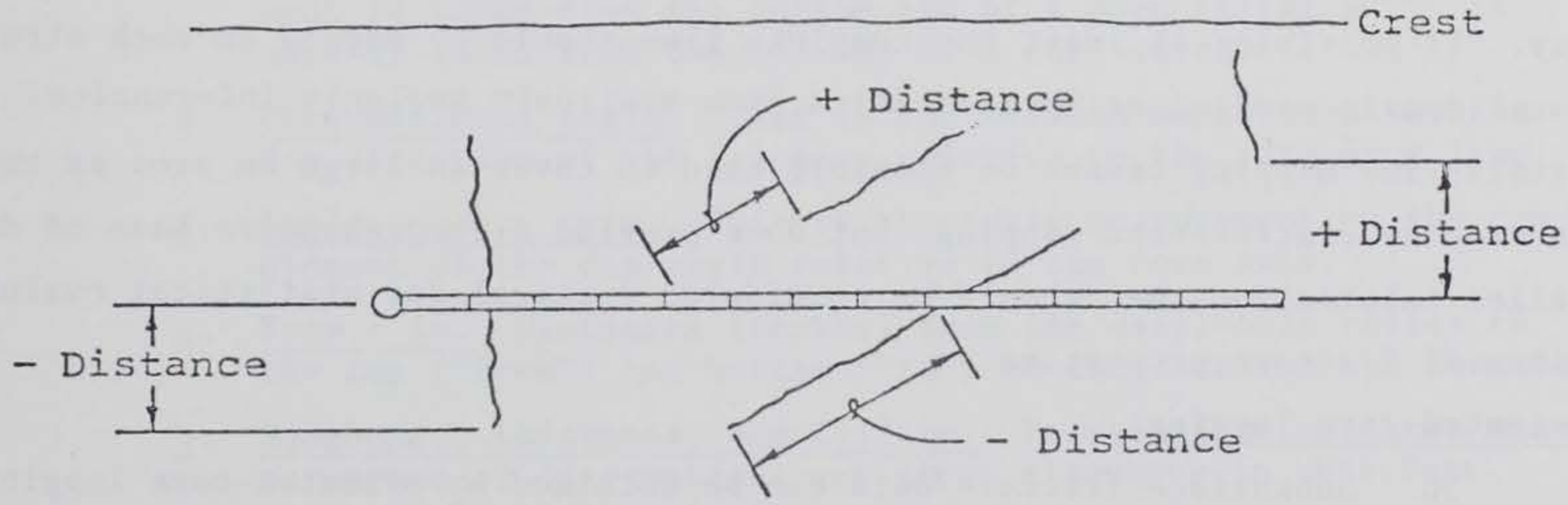

Figure 3. Illustration of field measurements for fracture overlap

i. Terminations. The manner in which a fracture terminates is described by a single alpha letter according to five designations: in rock, none, en echelon, high angle against another fracture, and low angle against another fracture (Figure 4).

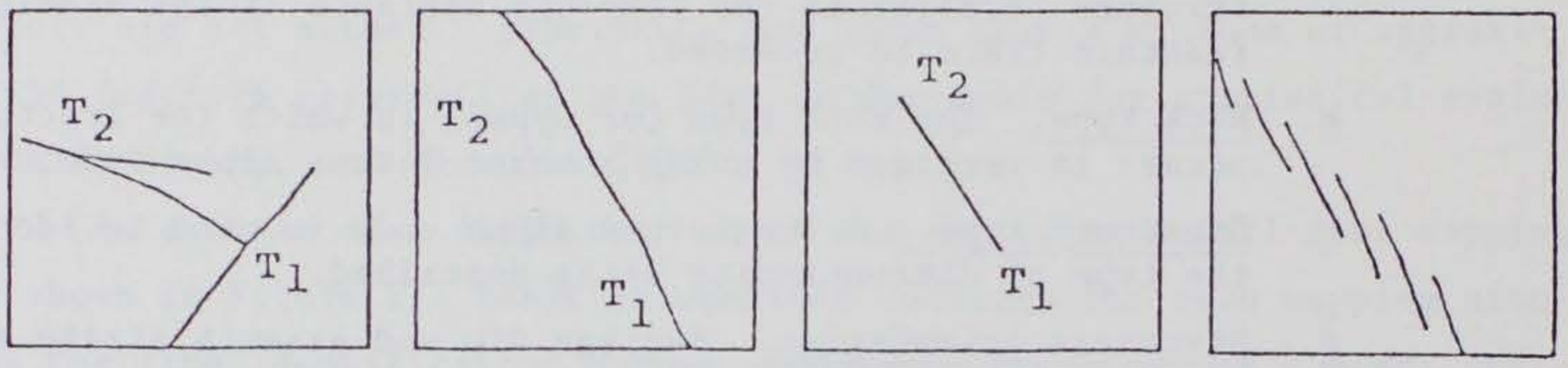

T_1 high angle > 20°	T_1 none	T_1 in rock	en echelon
T_2 low angle < 20°	T_2 none	T_2 in rock	

Figure 4. Various types of fracture terminations

j. Roughness. Roughness occurs on a scale of centimeters and is a qualitative rating (smooth, rough, or medium) of small irregularities on the fracture surface. A numeric rating can also be used, such as that suggested by the International Society for Rock Mechanics (1977).

k. Thickness. A thickness is recorded if separation occurs along the fracture.

l. Filling. Filling material (or materials) in the fracture opening is noted if present.

m. Water (W). The nature of water occurrence in the fracture (dry, wet, flowing, or squirting) is recorded using a single alpha letter.

29. For a typical mapping program in an area with accessible rock exposures a team of two experienced mappers working together (one taking measurements, the other recording data) can usually map two or three detail lines per day. If possible, at least one complete line should be mapped in each structural domain preliminarily identified from available geologic information. Detail-line mapping cannot be feasibly used to cover as large an area as that covered by fracture-set mapping, but does provide a comprehensive base of detailed information that should be considered critical for statistical evaluations of fracture properties.

Oriented-core logging

30. Subsurface fracture data can be obtained by oriented-core logging which provides a detailed record of fractures that intercept a diamond drill

hole. This type of data is similar to that of a very strict detail-line survey in which only those fractures intersecting the line are mapped.

31. Various devices and systems are currently available for orienting structural features in core holes. The most popular and reliable of these are the Christiansen-Hugel system, the Craelius core orientor, and an eccentrically weighted clay-imprint orientor. The latter two devices can only be used in inclined drill holes. The clay-imprint orientor as described by Call, Savely, and Pakalnis (1982) is by far the simplest, fastest, and least expensive device for orienting drill core. Its usage has a small effect on regular drilling rates and costs, usually causing only a 10 to 20 percent decrease in rates and a corresponding increase in costs.

32. An example of a field data sheet for recording oriented-core data from inclined drill holes is shown in Figure 5. Orientations of fractures in the drill core are measured relative to the core axis and to a reference line that has been scribed or drawn along the top edge of the core by the orienting device. These field measurements are made with a specially designed goniometer and later converted to true dip directions and dips by using vector mathematics and the drill-hole orientation.

33. For each fracture intercepted by the drill hole the following information is recorded on the illustrated data sheet:

a. Depth from start. The distance from the top of the drill run to the fracture occurrence is recorded. If 3-m drill runs are made, this distance will always be less than 3 m.

b. Rock type. The rock type (or types) in which the fracture occurs is recorded by using a three-letter alpha code.

c. Structure type. A two-letter alpha code is used to identify the type of discontinuity being described.

d. Top/bottom (T/B). A "B" is recorded if the goniometer measurement is taken from the bottom end of a core stick; a "T" is used if taken from the top end of a core stick.

e. Circumference angle. This is the azimuth measurement of the dip direction of the fracture relative to the reference line.

f. Angle to core axis. This is the angle measurement of the complement of the dip angle relative to the core axis.

g. From - to. Distances (depths) from the drill-hole collar to the top ("from") and bottom ("to") of the core run are recorded.

h. Roughness, thickness, and filling. Descriptions of these measurements or observations are given elsewhere in this Part.

34. Oriented-core data are appropriately used to supplement surface

IDENT NO. ☐☐☐☐☐☐☐☐ DATA SHEET FOR ORIENTED CORE PAGE ___ OF ___

HOLE NO. _____ LOCATION _____ IMPRINT AT _____ DATE _____ BY _____

COLLAR ELEV. _____ INCLINATION _____ BEARING _____ DIAM. _____

DEPTH FROM START (FT / M)	ROCK TYPE 1	ROCK TYPE 2	STRUCTURE TYPE	STRUCTURE T/B	STRUCTURE CIRCUM. ANGLE (DIP. DIR.)	STRUCTURE ANGLE TO CORE AXIS (DIP)	R	THICKNESS (IN / CM)	FILLING N	(FT / M) FROM	(FT / M) TO	COMMENTS

ROCK TYPE ABBREVIATIONS				STRUCTURE TYPE ABBREVIATIONS				FILLING ABBREVIATIONS				N	NONE
				SJ	SINGLE JOINT								
				FT	FAULT								
				CT	CONTACT								
								R=ROUGHNESS S,R					
								T/B = MEASUREMENT AT TOP OR BOTTOM OF CORE					
								B=DOWNHOLE					

Figure 5. Example of data recording sheet for oriented-core logging (from the Rock Mechanics Division of Pincock, Allen, and Holt, Inc., Tucson, Ariz.)

mapping data because fracture lengths cannot be measured in drill core. Another point to remember when analyzing core data is that measured fracture orientations tend to be more dispersed than those obtained from surface mapping because the core diameter limits the fracture area that can be observed and very little averaging subsequently occurs during the measurement process when compared to that for a fracture mapped in a surface exposure. Perhaps the greatest benefit of oriented-core logging is a resulting data base that allows for determining the subsurface extent of fracture sets and structural domains that are observed on the surface.

Display of Fracture Orientation Data

35. Before a suite of mapped fracture data can be statistically analyzed their orientations must first be displayed so that fracture sets and structural domains can be determined. The orientations are plotted on lower-hemisphere projections that display poles to fractures. Schmidt equal-area projections are commonly used because pole densities can be readily calculated and then contoured to help enhance fracture patterns (Figure 6). The blind zone shown in Figure 6 corresponds to the orientation of the mapped outcrop where fractures that parallel the outcrop are overlooked or sampled to a lesser degree than those with strikes mores perpendicular to the outcrop (Terzaghi 1965).

36. Schmidt plots derived from various mapping techniques are used in conjunction with knowledge of the local geology to help delineate structural domains in the study area. Fracture data are then combined within each domain and fracture sets critical to the slope design are identified. Geometric characteristics of the fracture sets can then be studied by generating histograms or cumulative distribution plots, from which probability density functions can be estimated for the characteristics. These estimated functions are required for probabilistic evaluations and analyses of rock slope stability.

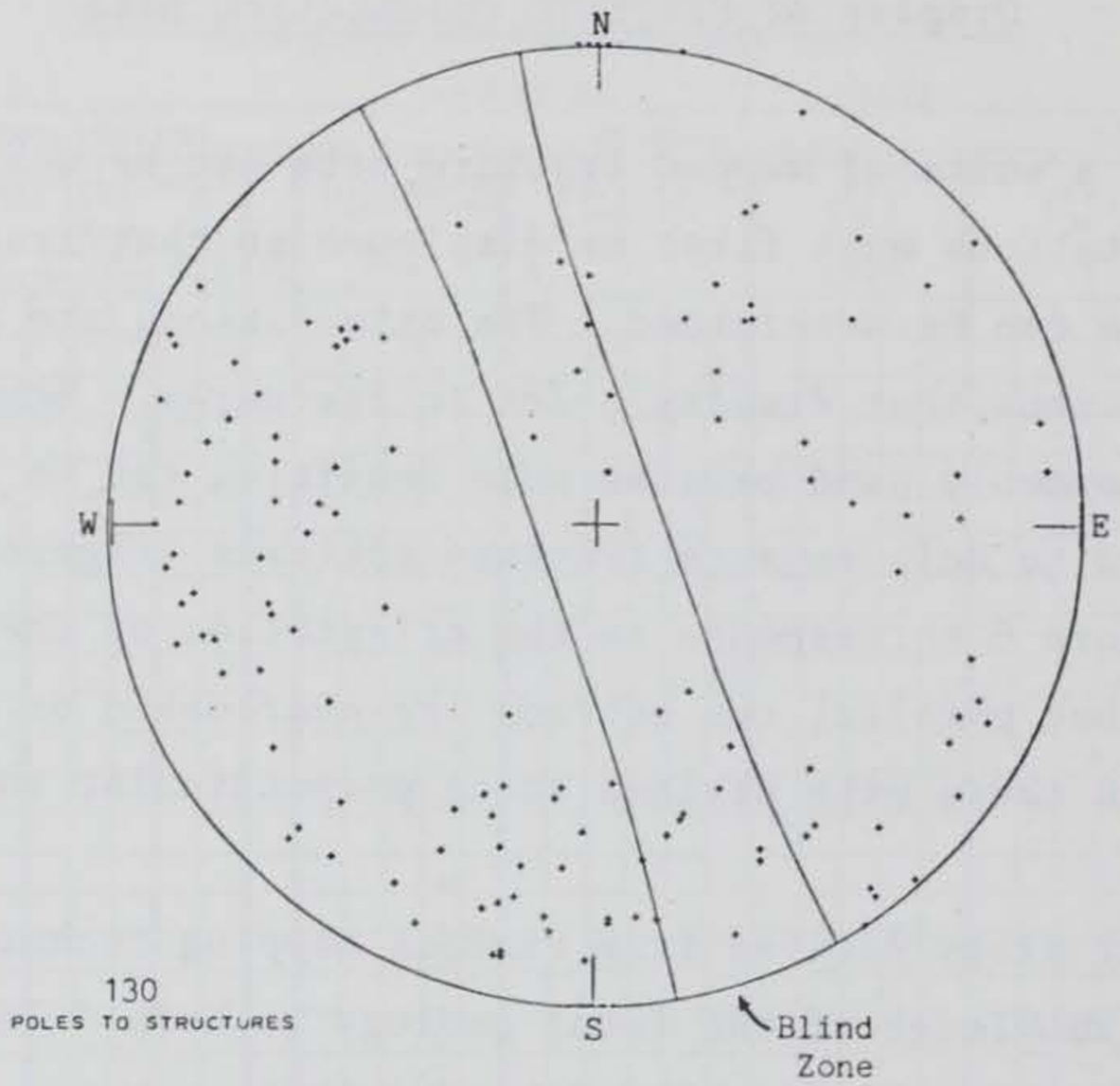

a. Point plot

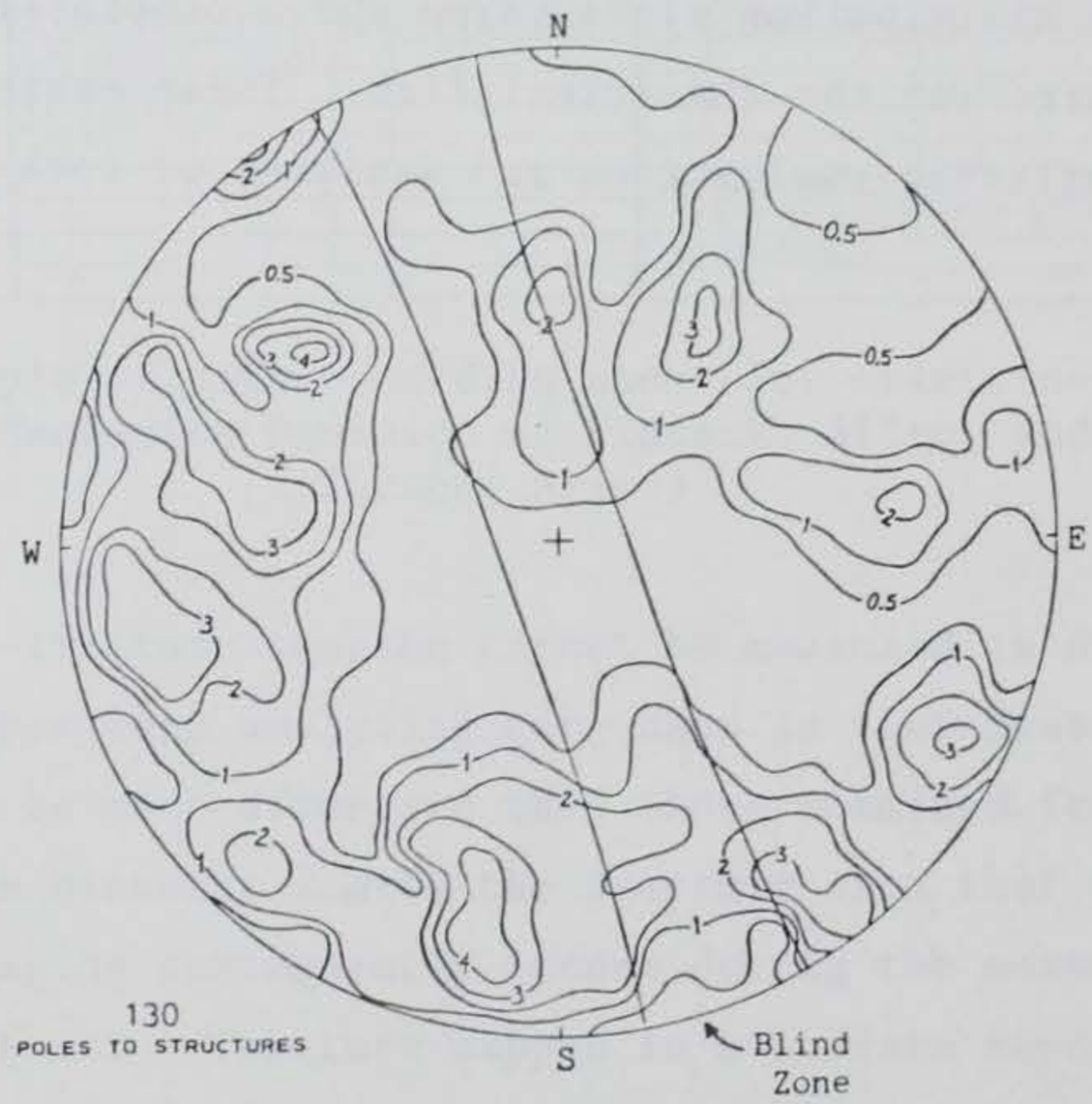

b. Contoured percent plot

Figure 6. Lower-hemisphere Schmidt plots of mapped fracture orientations obtained from a detail-line site

PART III: STATISTICAL ANALYSIS OF FRACTURE DATA

37. Mapped fracture orientations displayed on Schmidt plots provide the foundation for analyzing fracture data for probabilistic slope engineering. Plots obtained from various mapping sites are used to help delineate structural domains and to identify and describe fracture sets within each domain. After sorting the data according to sets, the fracture properties for each set are analyzed to obtain estimates of their probability distributions and spatial correlations.

Delineation of Structural Domains

38. The delineation of structural domains is essential to rock engineering studies because geologic and hydrologic properties vary from one domain to another. Obvious domain boundaries correspond to lithologic contacts caused by fault displacement, intrusion, or depositional environment. However, structural domain boundaries are not restricted only to lithologic contacts, but may also occur within the same rock unit. These less obvious boundaries often can be determined by visually comparing Schmidt plots that display fracture orientations from various mapping sites.

39. Preferred fracture orientations appear as clusters of poles on a Schmidt plot. Each cluster represents a fracture set, and the spatial relationships of clusters on the plot allow for meaningful visual comparisons with other plots. In the evaluation of two or more plots geologic experience and judgment provide the basis for determining whether the plots are alike and, thus, represent samples from the same structural domain.

40. If fracture orientations appear dispersed and random on the plots with no obvious clustering, then visual comparisons are not appropriate, and quantitative, statistical methods are needed to evaluate the plots and provide guidance in locating structural domain boundaries. A chi-squared testing procedure has been adapted to the comparison of Schmidt plots and provides a way to evaluate one's confidence in claiming that two or more plots were obtained from the same structural domain (Miller, 1983). The procedure is based on the analysis of a contingency table that contains frequencies of fracture poles that occur in corresponding patches on the Schmidt plots being compared (Figure 7).

Rows	Patch 1	Patch 2	Patch 3 . . .	Patch c	Row Total
Schmidt Plot 1	f_{11}	f_{12}	f_{13} . . .	f_{1c}	R_1
Schmidt Plot 2	f_{21}	f_{22}	f_{23} . . .	f_{2c}	R_2
Schmidt Plot 3	f_{31}	f_{32}	f_{33} . . .	f_{3c}	R_3
.	.	.	.	.	.
.	.	.	.	.	.
.	.	.	.	.	.
Schmidt Plot r	f_{r1}	f_{r2}	f_{r3} . . .	f_{rc}	R_r
Column Totals	C_1	C_2	C_3 . . .	C_c	N

Figure 7. Arrangement of contingency table for comparing Schmidt plots

41. In the contingency table, samples from r structural populations (domains) are listed down the rows in terms of the Schmidt plots. Each sample is classified into c categories, or patches. The frequency of observed fracture poles in the ij cell (i^{th} plot, j^{th} patch) is denoted by f_{ij}. To test the null hypothesis that the plots represent samples from like populations, the following statistic is calculated:

$$\chi^2 = \sum_{i=1}^{r} \sum_{j=1}^{c} \frac{(f_{ij} - e_{ij})^2}{e_{ij}} \qquad (1)$$

where

r = total number of Schmidt plots

c = total number of patches in each plot

f_{ij} = observed frequency of fracture poles in the ij cell

e_{ij} = expected frequency of fracture poles in the ij cell

The expected frequency in the ij cell is calculated as follows:

$$e_{ij} = \frac{R_i C_j}{N} \qquad (2)$$

where

R_i = total observed frequency of poles in the i^{th} row

C_j = total observed frequency of poles in the j^{th} column

N = total number of fracture observations in all plots

42. If the null hypothesis is true, then the above statistic is chi-squared distributed with (r-1)(c-1) degrees of freedom (provided each fracture is sampled independently of other fractures), and its value does not exceed that of a chi-squared variate evaluated at a specified significance level α. The value of α is actually equivalent to the area under a chi-squared distribution to the right of its associated χ^2 value. The usual test procedure consists of selecting an α value and then calculating the value of χ^2 from the contingency table. The null hypothesis is rejected if this calculated value exceeds the known tabulated value of χ^2 with (r-1)(c-1) degrees of freedom for the specified α.

43. However, rather than selecting a particular significance level for comparing Schmidt plots, it is often desirable from a geologic standpoint to use the calculated χ^2 value from the contingency table to compute its corresponding right-tailed area α. This computed α value is not really a level of significance but serves as a measure of one's confidence in accepting the null hypothesis, providing a quantitative and standardized measure of comparison among different contingency table analyses of Schmidt plots. A numerical procedure for estimating the right-tailed area under a chi-squared distribution with more than 30 deg of freedom is given by Zelen and Severo (1965).

44. In summary, contingency table analysis is a useful tool for comparing Schmidt plots and evaluating the similarity of sampled structural populations. The method is intended for plots that display dispersed fracture orientations where the lack of well defined clusters makes visual comparisons difficult and often useless. The necessary statistical calculations can be easily programmed on a desk-top computer, thus providing for a rapid way to compare Schmidt plots obtained from various mapping sites. Such comparisons are important for helping to predict the locations of structural domain boundaries.

Combining Fracture Data from Different Mapping Sources

45. In fracture mapping programs for many slope design projects various

mapping techniques are employed at different sites. After structural domains have been delineated in the study area, these mapped fracture data can be combined by domain to provide a foundation for the statistical analysis of fracture set properties in each domain.

46. One of the first steps in combining fracture data is the delineation of fracture sets on each of the Schmidt plots. If fracturing is complex within a structural domain and preferred orientations are not readily seen in the plots, the density of fracture poles in small counting areas can be contoured to assist in the visual identification of fracture sets. Statistical methods are also available to help analyze and distinguish clusters of orientations on a given plot (Shanley and Mahtab 1976, and Mahtab and Yegulalp 1982). However, objective statistical analyses are strictly numerical and do not include engineering judgment that can often make identifying fracture sets from careful observations of rock exposures possible. An experienced investigator who has mapped the fractures in an outcrop and has knowledge of slope design procedures and requirements can apply geologic information practically impossible for a statistical analysis to include. Therefore, statistical methods are tools that should guide rather than control in the delineation of fracture sets.

47. Because mapping methods and outcrop orientations often vary from one mapping site to another, observations of individual sets are analyzed separately to evaluate their characteristics. For instance, measured spacings in a given fracture set as mapped by detail-line techniques are corrected to true spacings by using the mean orientation of the set and the orientation of the mapping line. This correction is different for each observation of the set (denoted as a subset) and for each mapping line.

48. The mean vector of a mapped fracture subset is not only useful for the spacing correction but also can be used to explicitly describe the mean orientation of the subset and to aid in combining numerous fracture data obtained from different sites within a structural domain. This vector represents the average direction of normals to fracture planes in the given subset and, if plotted as a pole, indicates the "center" of the Schmidt cluster that represents the observed fracture set. The normalized mean vector of a given fracture set is calculated by using the following expression:

$$\underline{V}_m = \frac{1}{\sqrt{\left(\sum_{i=1}^{N} x_i\right)^2 + \left(\sum_{i=1}^{N} y_i\right)^2 + \left(\sum_{i=1}^{N} z_i\right)^2}} \begin{bmatrix} \sum_{i=1}^{N} x_i \\ \sum_{i=1}^{N} y_i \\ \sum_{i=1}^{N} z_i \end{bmatrix} \quad (3)$$

where

$\underline{V}_m$ = mean vector of fracture set

N = total number of fractures in the set

x_i, y_i, z_i = direction cosines of a normal to the i^{th} fracture

49. The plane orientation perpendicular to the mean vector is often truncated to serve as an abbreviated identifier for the fracture set. For instance, a mean-vector plane with a dip direction of 162 deg and a dip of 47 deg would be labeled as 16.4. All the set mean vectors from different mapping sites within a given structural domain can then be plotted on a single lower-hemisphere projection to aid in the grouping of fracture subsets (Figure 8).

50. Fracture set properties are combined directly if the same mapping technique was used for each subset in a given group. Thus, all the observations are pooled and treated as independent samples for calculating means and standard deviations and for estimating probability distributions. However, if different mapping methods were used, then weighted means are calculated according to the number of fracture observations in each subset and probability distributions are inferred from experience with other similar type data. Selected fracture set properties taken from the data represented by Figure 8 are briefly summarized in Table 1.

Probability Distributions of Fracture Set Properties

51. The combined fracture data for a given structural domain constitute samples of the fracture set properties in that domain. These sample data can be used to construct histograms or cumulative frequency plots for pertinent properties in each fracture set. These plots are then used to help determine the probability distributions that best describe the mapped fracture properties. Statistical "goodness of fit" tests can also be used in this evaluation process.

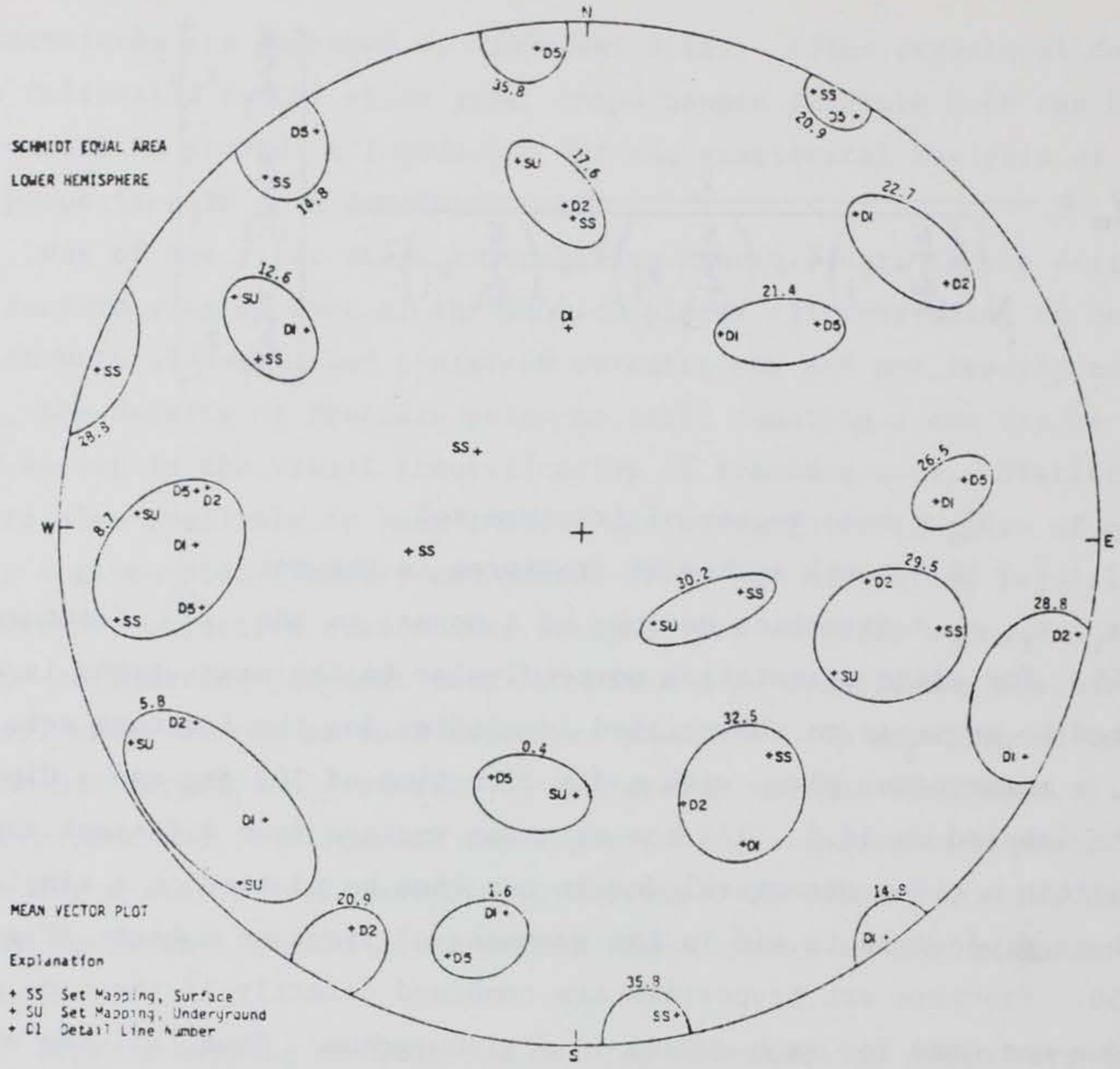

Figure 8. Mean vector plot showing the grouping of fracture subsets for a specified structural domain

Table 1

Partial Listing of Fracture Set Properties for the Structural Domain Represented by Figure 8

Fracture Set No.	No. of Observations	Dip Direction, deg Mean	Dip Direction, deg S.D.*	Dip, deg Mean	Dip, deg S.D.	Length Mean, ft	Spacing Mean, ft	Waviness Mean deg
0.4	23	5.7	9.7	42.6	8.2	2.5	0.8	2.3
1.6	39	12.0	10.2	66.9	12.4	2.4	0.5	9.1
5.8	56	50.9	9.7	82.6	10.2	3.2	0.9	3.1
8.7	149	88.2	12.9	74.9	9.9	4.0	1.1	3.9
12.6	30	122.9	10.8	67.3	11.6	3.1	1.0	0.4
17.6	36	171.5	9.8	62.3	7.2	2.7	0.9	1.6
26.5	25	261.0	8.4	61.3	15.0	4.7	0.9	4.2
28.8	22	288.5	11.3	86.9	8.4	2.2	1.4	5.4
29.5	134	291.3	9.8	52.2	12.5	3.3	1.6	1.5
32.5	23	328.5	12.4	51.7	12.6	2.1	0.7	3.6

* S.D. = Standard deviation.

52. Distributions of dip and dip direction are usually best approximated by normal distributions (Figure 9), although some fracture sets may have orientation data that are nearly uniformly distributed. Distributions of set spacing, length, and waviness are typically approximated by exponential distributions (Robertson 1970; Call, Savely, and Nicholas 1976; and Cruden 1977) as shown by the examples in Figure 10. However, some investigators report that trace lengths within a fracture set may be distributed in a lognormal fashion (McMahon 1974, Bridges 1976, and Baecher et al. 1978).

53. Statistical treatment of mapping bias and the censoring of fracture length traces have been discussed by Baecher (1980) and Laslett (1982). Such methods are used to adjust the distributions of mapped fracture lengths to provide improved estimates of the true length distributions.

54. Probability distributional forms other than those indicated above may occasionally be used to best describe the distributions of mapped fracture set properties. Regardless of which particular form may be used, the basic requirements are that it be a valid probability density function that can be explicitly expressed and that it be amenable to subsequent slope stability analyses.

Spatial Correlations of Fracture Set Properties

55. A fracture property within a given set tends to be spatially correlated, and geostatistical methods can be used to determine the nature and extent of the correlation (Miller 1979, and La Pointe 1980). In classical statistics the samples collected to describe an unknown population are assumed to be spatially independent (that is, knowing the value of one sample does not provide any information about adjacent samples). In contrast, geostatistics is based on the assumption that adjoining samples are spatially correlated and that the nature of the correlation can be statistically and analytically expressed in a function called the variogram function (Matheron 1963).

56. In the analysis of fracture set properties weak second-order stationarity is assumed and estimates of the variogram functions are computed along the mean vector line of each fracture set (Miller 1979). A given variogram function is estimated from sample data along a line according to:

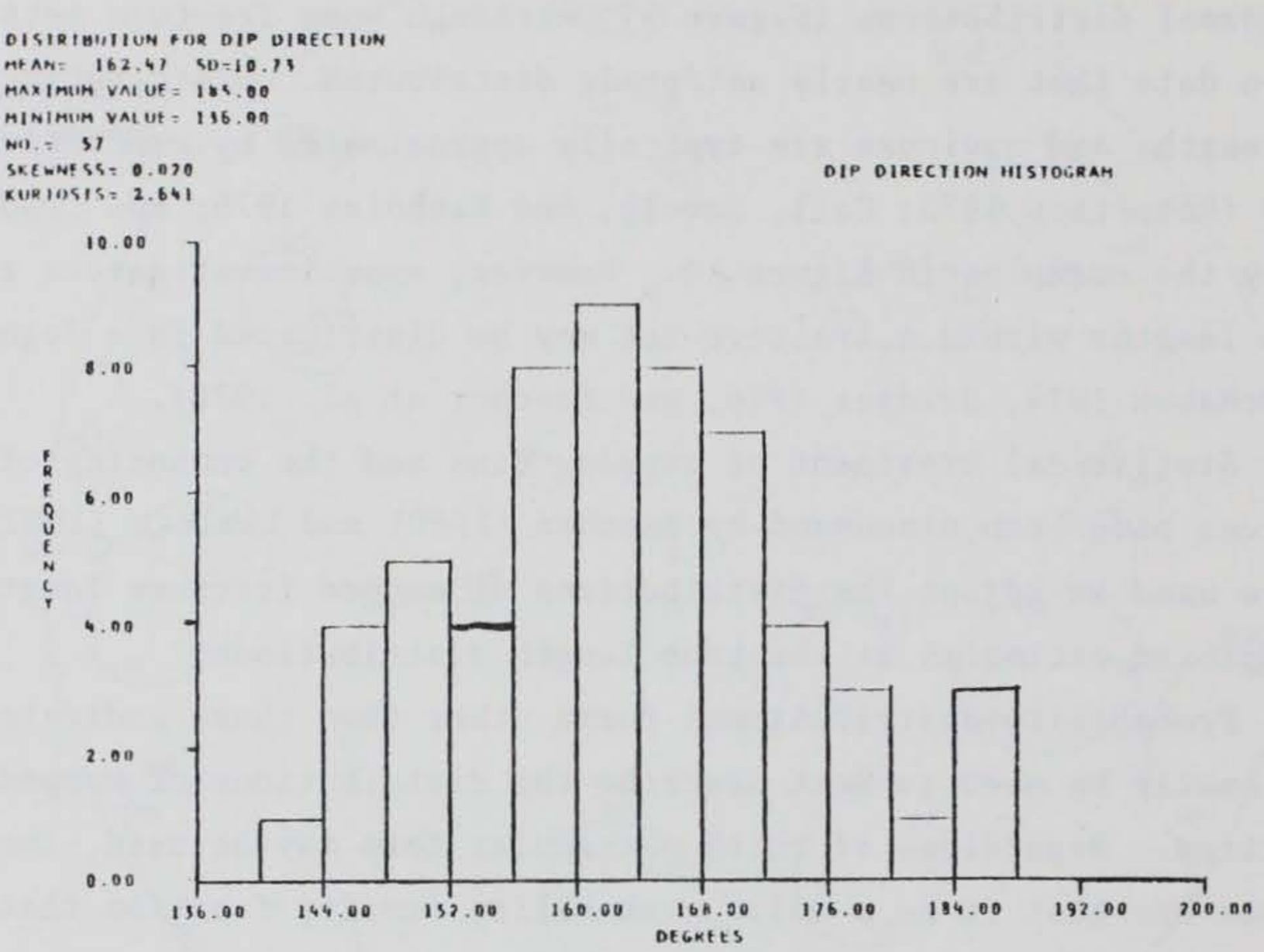

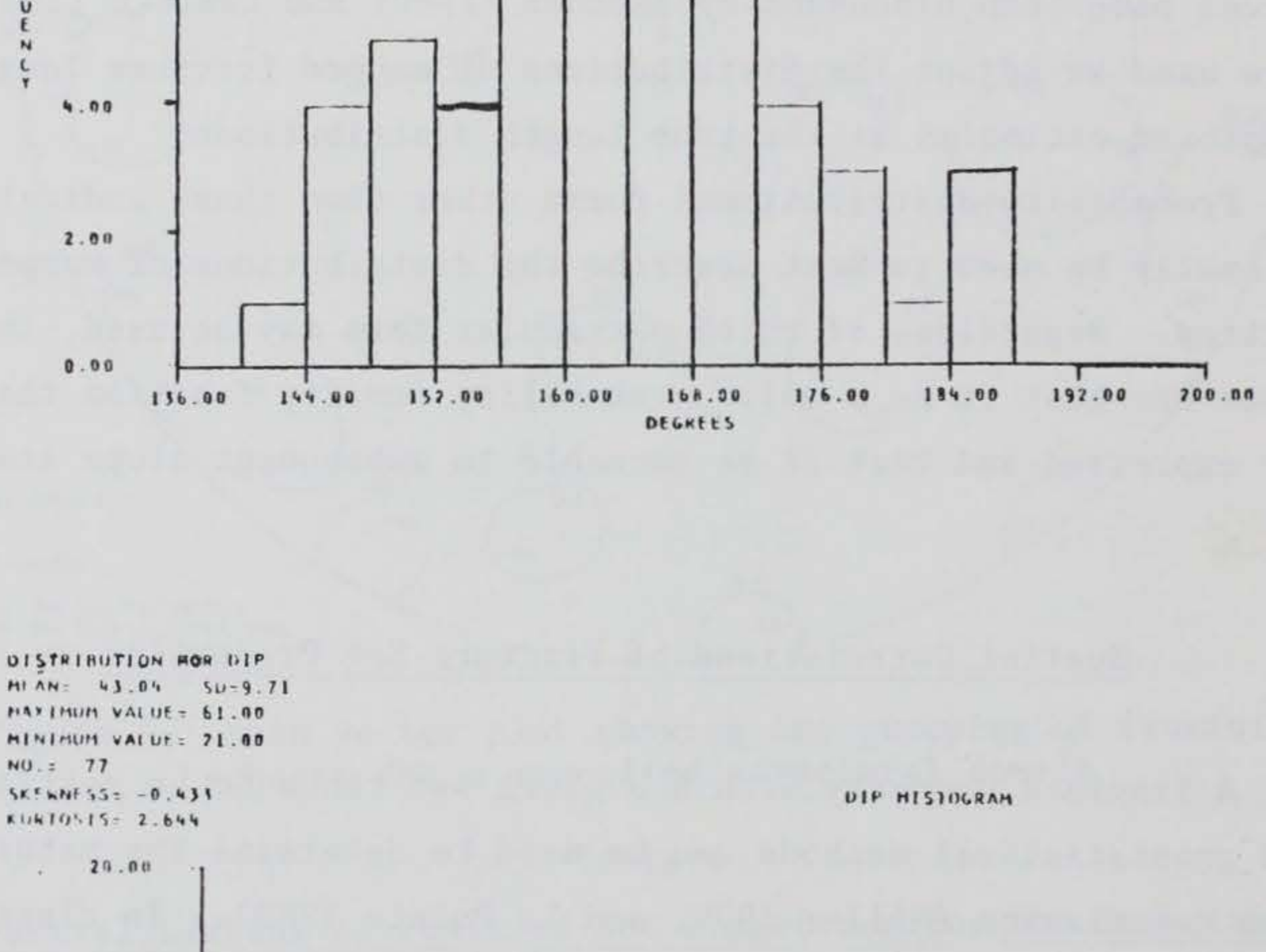

Figure 9. Typical histograms of fracture set dip direction and dip that indicate normal distributions

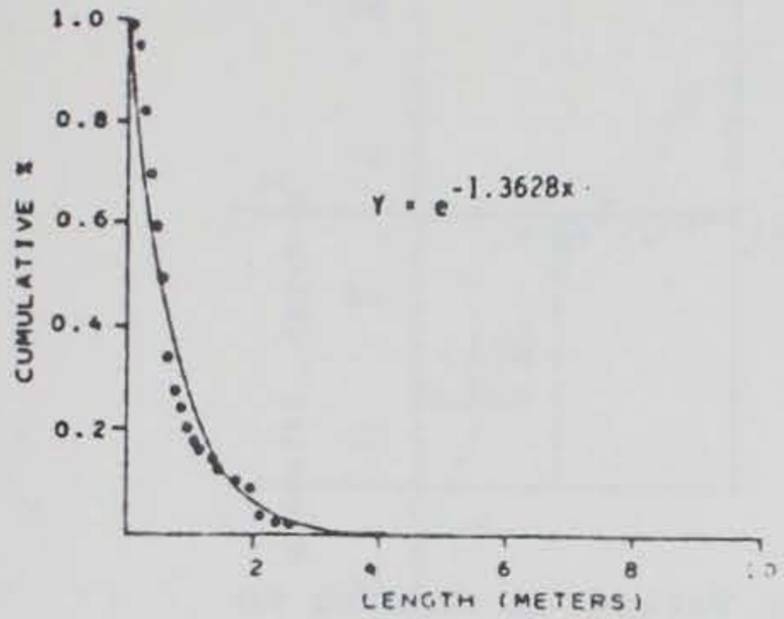

A. Typical Length Distribution

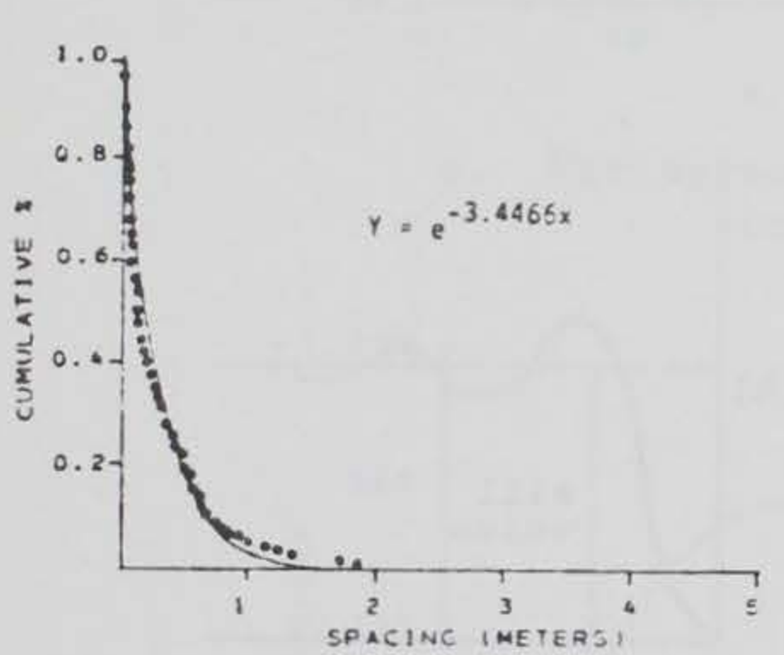

B. Typical Spacing Distribution

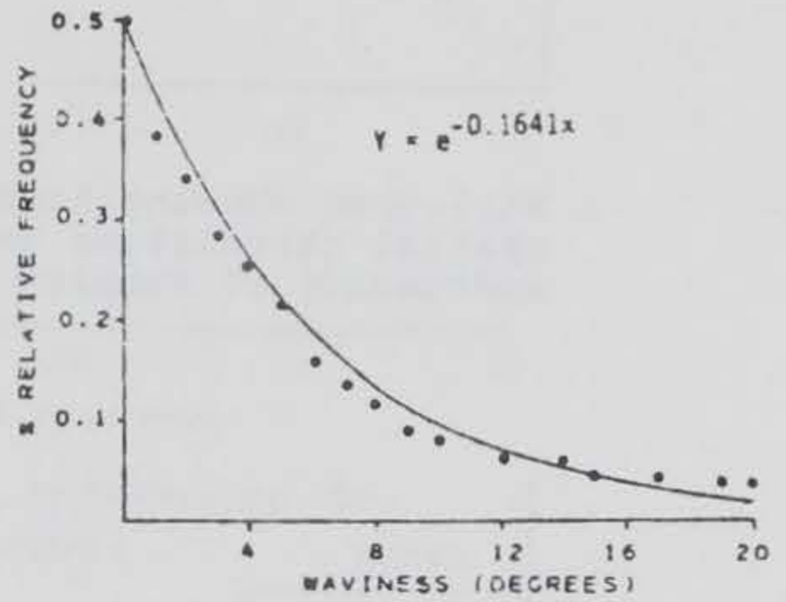

C. Typical Waviness Distribution

Figure 10. Examples of exponential distributions of fracture set length, spacing, and waviness (from Call, Savely, and Nicholas 1976)

$$\hat{\gamma}(h) = \frac{1}{2N} \sum_{i=1}^{N} \left[Z(x_i) - Z(x_i + h) \right]^2 \qquad (4)$$

where

N = total number of sample values

$Z(x_i)$ = sample value at location x_i

$Z(x_i + h)$ = sample value at location $x_i + h$

The estimated function, $\hat{\gamma}(h)$, is expressed in a graph with h plotted as the independent variable. For fracture set data the distance h can either be measured in terms of actual distance or in terms of fracture number. At least 30 samples should be used in estimating the function in most cases.

57. Examples of variograms and theoretical variogram models are shown in Figure 11. For the spherical model the value of $\gamma(h)$ at the point where the curve reaches a plateau is called the sill value and the corresponding value of h is called the range. The sill value equals the variance of all

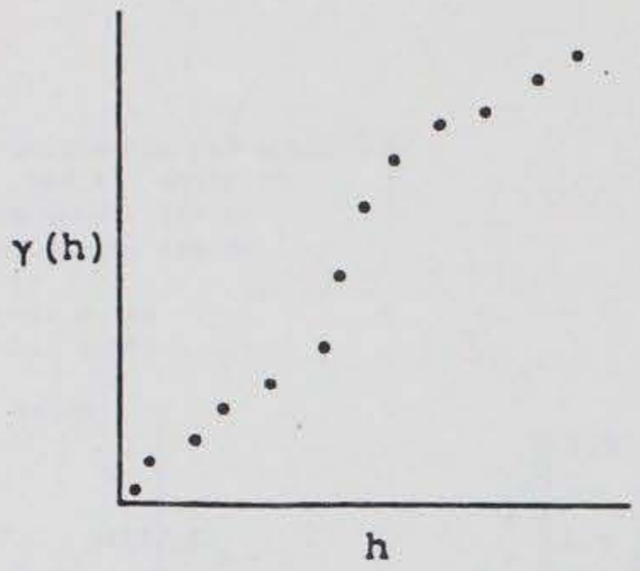

a. Variogram showing high spatial correlation and continuity of samples

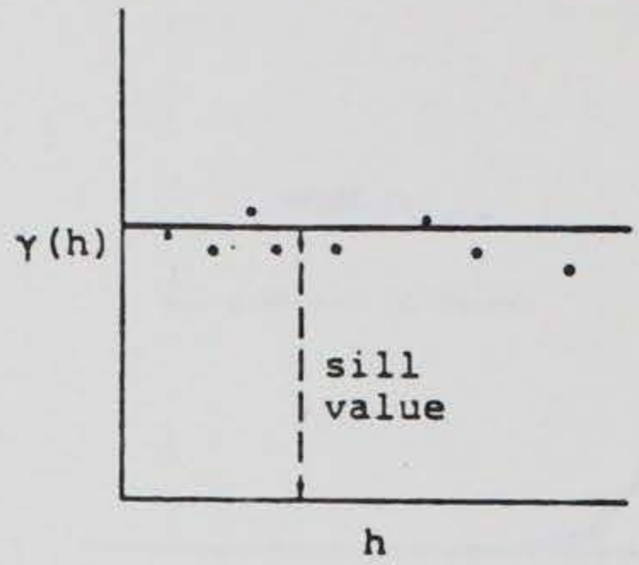

b. Variogram showing no spatial correlation of samples

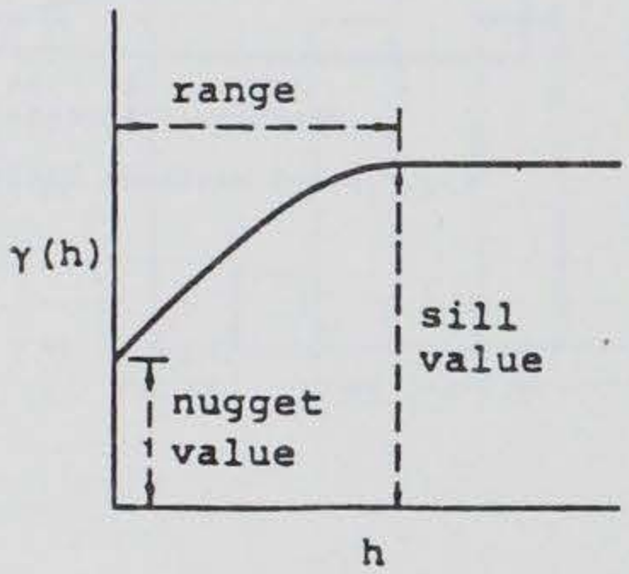

c. Theoretical spherical model showing some spatial correlation of samples

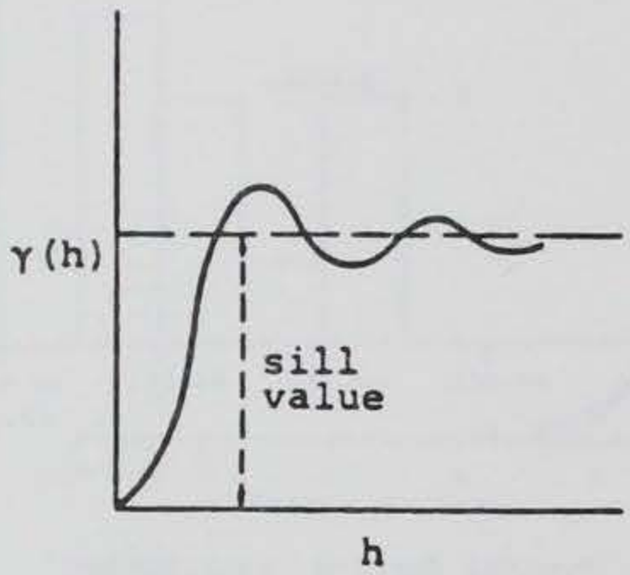

d. Theoretical hole-effect model showing spatial correlation of periodic samples

Figure 11. Examples of variograms and theoretical models

sample values used in calculating the variogram. The range can be considered in the traditional geologic concept of range of influence (that is, any two samples spaced further apart than this distance are not spatially correlated). Thus, the variogram represents a measurement of correlation as distance between samples increases. The value of $\gamma(h)$ at h equal to zero is known as the nugget value. Ideally, the nugget should be zero because any two samples from the same point should have equal values. However, a nugget practically always occurs in variograms of geologic data and may indicate highly erratic sample values spaced at close distances or may reflect errors or uncertainties in sample collection and evaluation.

58. Typical variograms for fracture set properties are illustrated in Figure 12. For most fracture sets the spherical model is appropriate for describing the spatial relationships of a specified fracture property. If

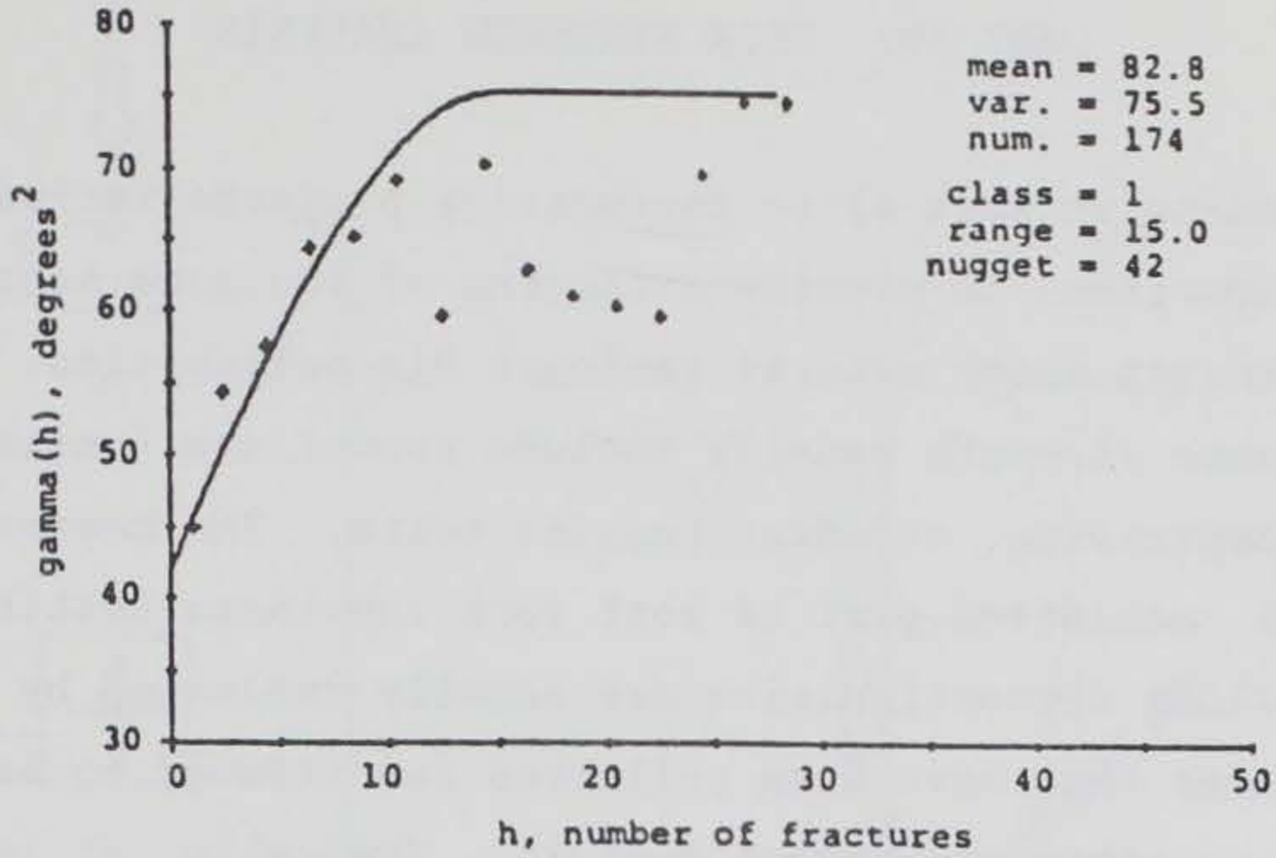

a. Variogram of dip referenced to fracture number

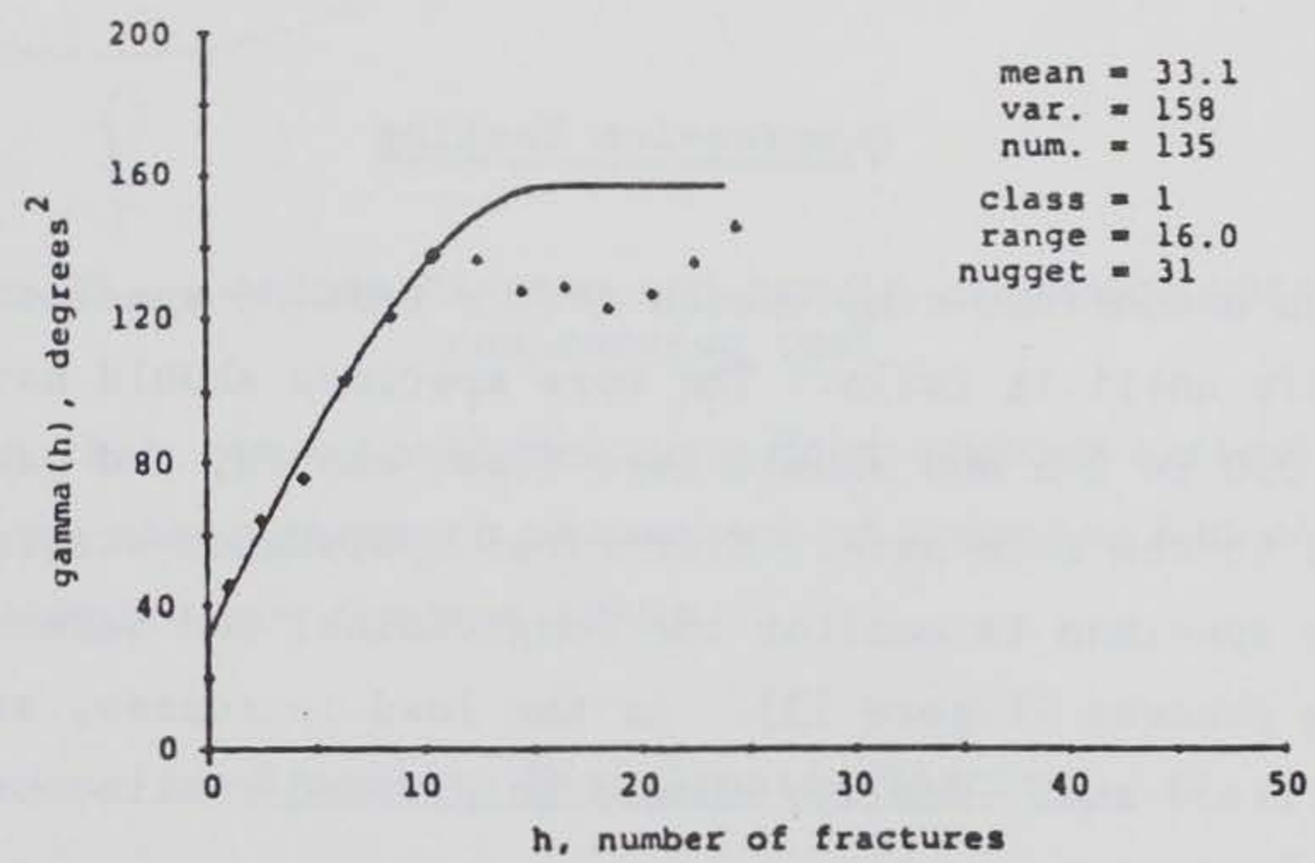

b. Variogram of dip direction referenced to fracture number

Figure 12. Example variograms of fracture set properties (from Miller 1979)

periodicity is indicated, then a modified hole-effect model can be used (Miller 1979).

PART IV: ROCK STRENGTH ANALYSIS

59. Comprehensive rock slope engineering projects include laboratory testing of rock specimens to provide estimates of the rock substance strength and the shear strength along natural geologic discontinuities. Tests for evaluating substance strength usually include unconfined (uniaxial) compression, triaxial compression, and disc tension tests. The measurement of rock densities is also considered part of most rock substance testing programs. Shear strengths along discontinuities are usually evaluated by direct shear testing of specimens that have been collected and trimmed so as to contain a natural fracture or other structural feature. Typically, at least four to six specimens of each rock type in the study area are desired for each kind of laboratory test.

Compression Testing

60. In an unconfined compression test a trimmed specimen of drill core is loaded axially until it fails. The core specimen should have a length-to-width ratio of 2.0 to 2.5 and should have flat, smooth, and parallel ends cut perpendicularly to the core axis. Electrical resistance strain gauges can be attached to the specimen to monitor the longitudinal and lateral strains during the loading process (Figure 13). As the load increases, signals from the gauges are amplified and, ideally, should be plotted continuously by a graph recorder.

61. The unconfined compressive strength is calculated by dividing the failure load by the cross-sectional area of the specimen. The elastic moduli are calculated using the graphs produced by the strain gauge output. Young's modulus, E, is the ratio of axial stress to longitudinal (axial) strain. Poisson's ratio, ν, is the ratio of lateral strain to longitudinal strain.

62. A triaxial compression test is similar to an unconfined test except the rock specimen is laterally confined, usually by a stress applied by hydraulic pressure. The specimen is sheathed in an impermeable membrane and placed in a hydraulic cell. By raising the cell pressure to a predetermined stress level, the specimen is subjected to a constant overall confinement. An axial load is applied by a ram and is increased until the specimen fails. Several tested specimens of the same rock type provide values of failure and

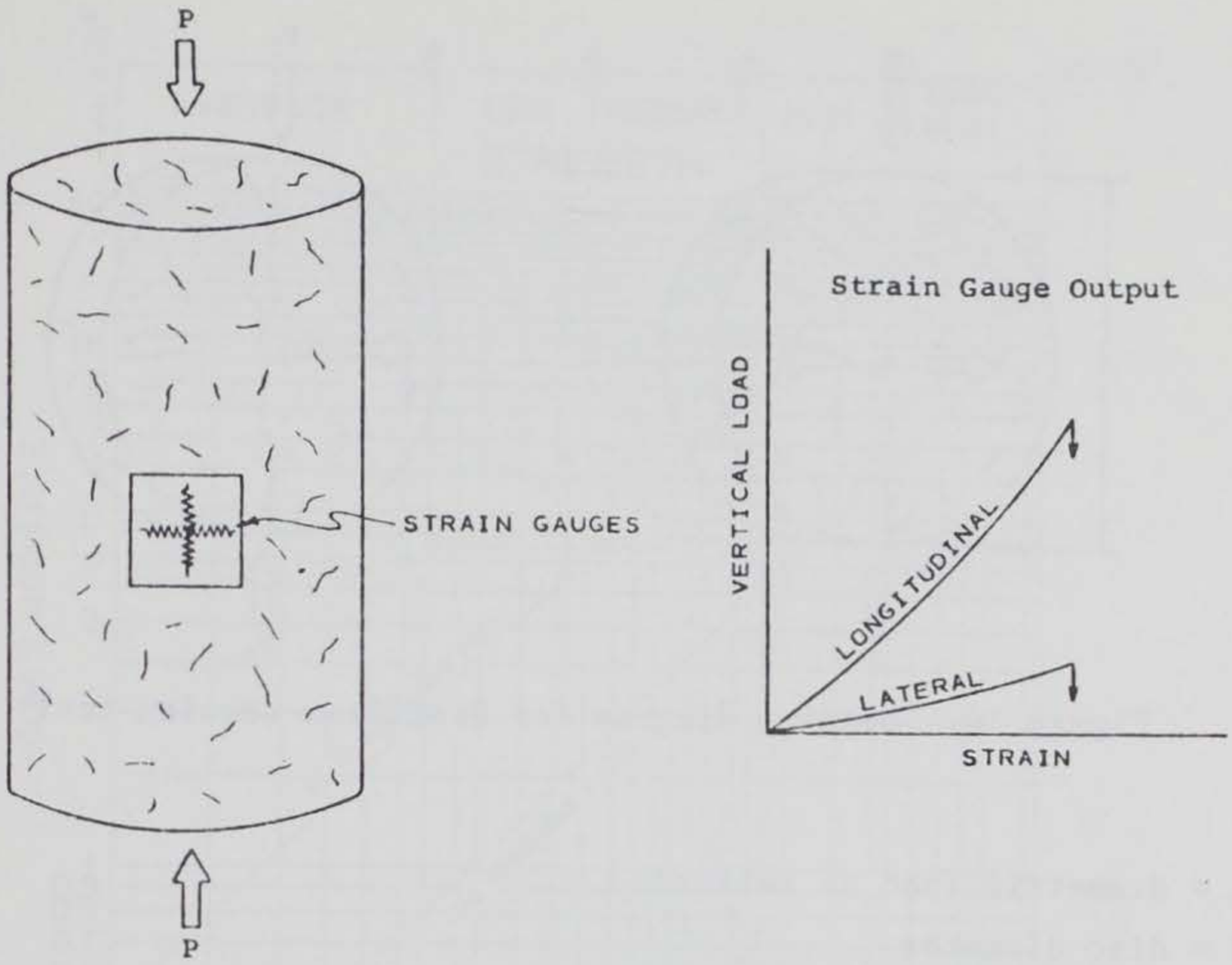

Figure 13. Loading diagram and strain graph for unconfined compression test

confining stress that can be analyzed in a Mohr-Coulomb criterion to provide the rock substance shear strength parameters of cohesion and coefficient of friction (for example, see Goodman 1980).

Brazilian Disc Tension Testing

63. Brazilian disc tension testing is convenient for estimating rock substance tensile strength. The testing procedure consists of diametrically loading a disc of drill core until it fails. The diametric load, P, effectively induces a tensile stress, σ_3, perpendicular to the loading direction (Figure 14). The load at failure, P_f, is noted when the rock disc shows visible signs of cracking and an inability to carry load. The tensile strength of the specimen, T, is calculated by the following equation:

$$T = \frac{2P_f}{\pi dh} \tag{5}$$

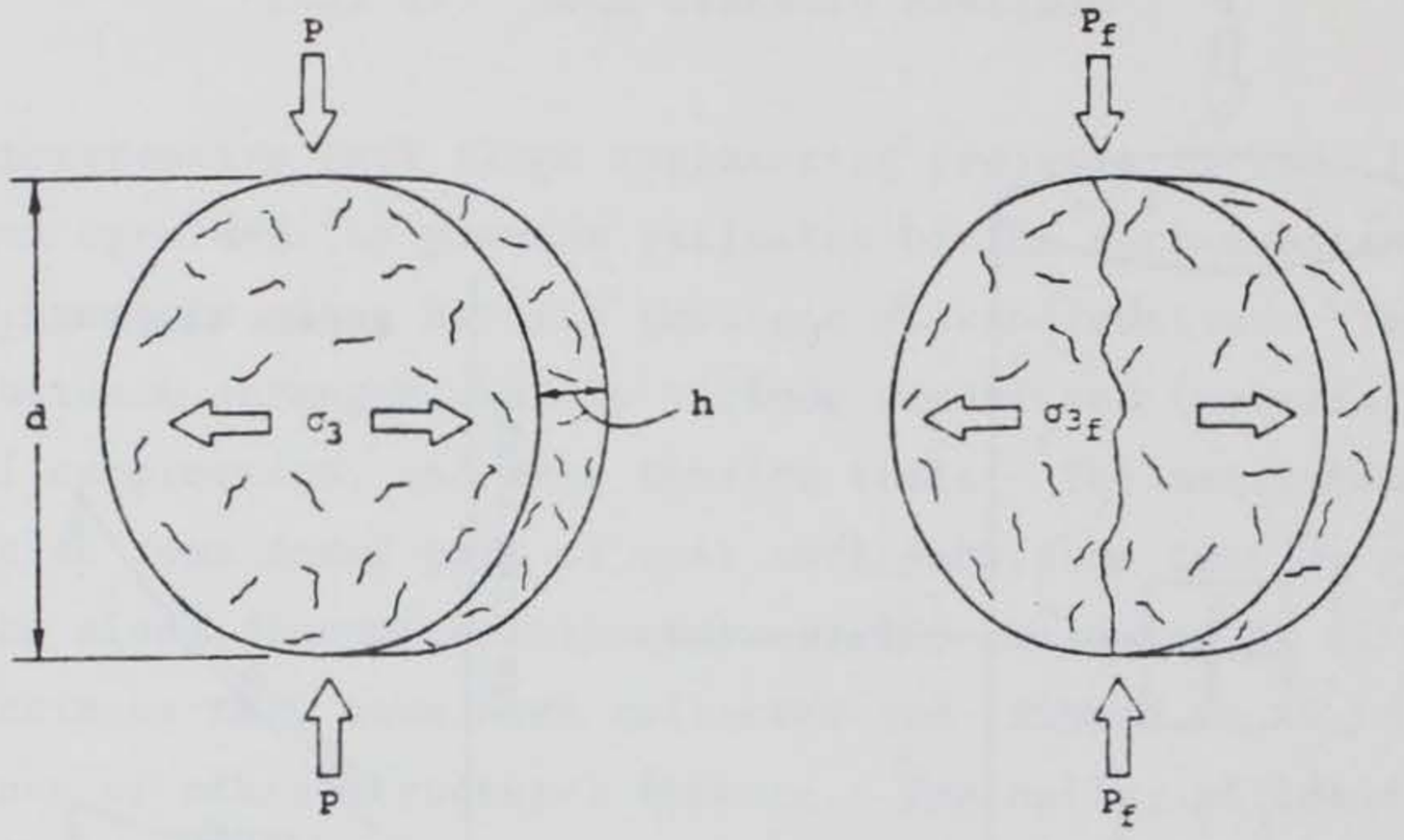

Figure 14. Loading diagram for Brazilian tension test

where

P_f = diametric load at failure

d = disc diameter

h = disc thickness

64. Tensile strengths estimated by Brazilian testing are assigned to the rock substance unless the specimen fails along an apparent surface of weakness. One major advantage is that it is much easier to prepare and load specimens for this type of test than to arrange the precise alignment and end preparation required for a direct tensile test.

Rock Substance Classification and Rock Quality Designation

65. Major rock types within a study area can be classified according to an accepted engineering scheme (Deere 1968) based on results of uniaxial compression tests (see example in Figure 15). This classification scheme is useful for comparing and characterizing different rock substances.

66. Rock quality designation (RQD) measurements of drill core provide another means of comparing different rock types. RQD is an indirect measure of fracture frequency and is evaluated by determining the percent recovery of core in lengths greater than twice its diameter (Goodman 1980). As an example, for NX core the RQD is calculated by summing the lengths of all core pieces longer than 10 cm and dividing that sum by the total length of the respective drilling interval (usually 3 m).

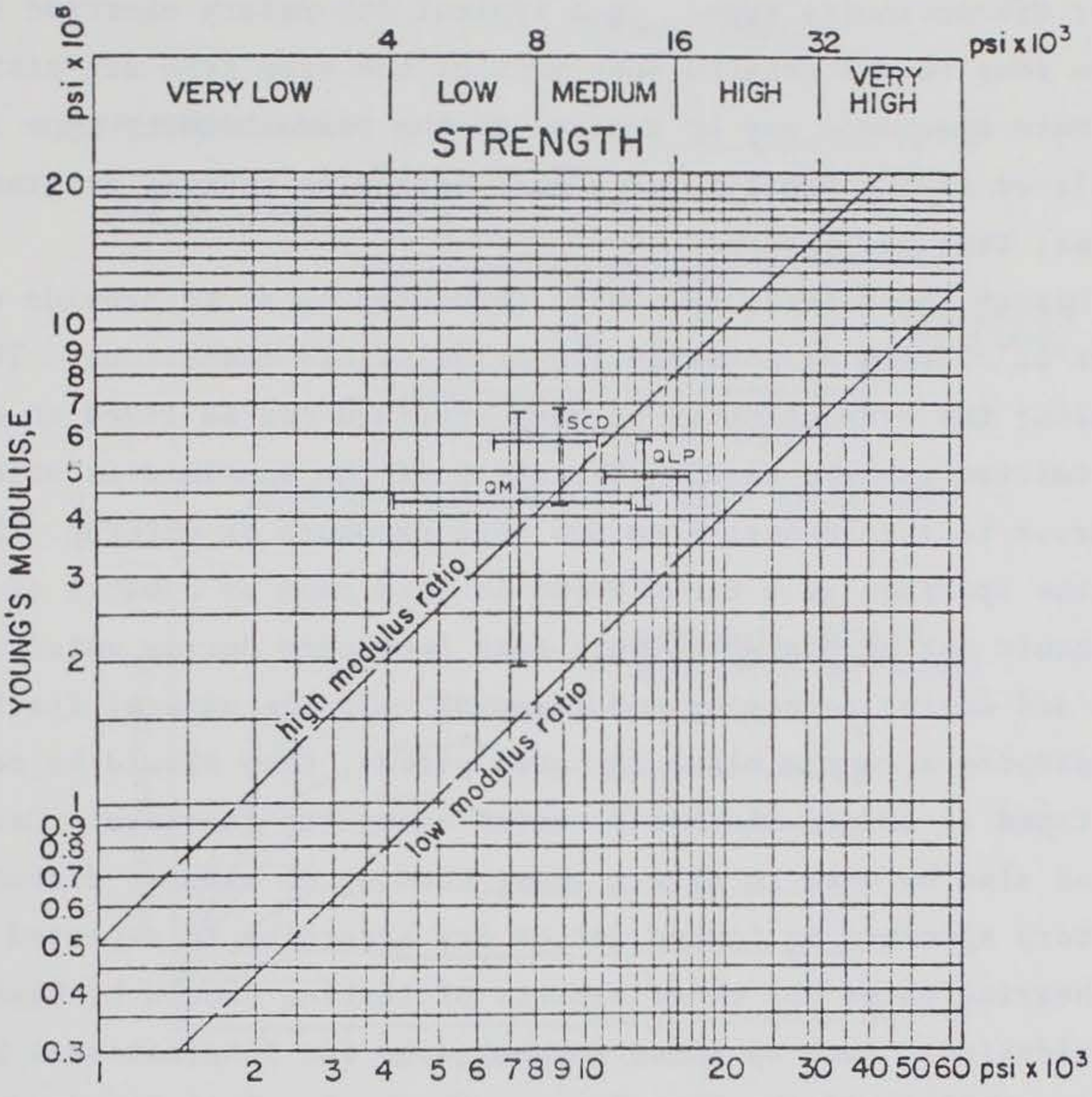

Figure 15. Example of rock substance classification for three different rock types (To convert pounds per square inch (psi) to pascals, multiple by 6894.757.)

67. Rock substance strength influences core breakage, and thus, affects RQD measurements. A low RQD value indicates either closely spaced fractures, low rock strength, or both. A high RQD value indicates either widely spaced fractures, high rock strength, or both.

Direct Shear Testing

68. The estimation of shear strengths along geologic discontinuities that form potential failure surfaces is essential in the engineering analysis of rock slope stability. Shear strengths are usually evaluated in the laboratory by direct shear testing of oriented rock specimens collected at the project site. A probabilistic stability analysis requires that the measurement uncertainty and natural variability of shear strength be quantified for each

rock type or discontinuity type. In a typical laboratory exercise the test results from four to six sheared specimens of the same type are statistically combined. More specimens may be desired if the discontinuity type is especially variable or if the benefits of a more extensive testing program warrant the additional time and expense.

69. Direct shear tests should be conducted so as to provide conditions that reflect as closely as possible the actual field conditions. The shearing direction along the discontinuity in each specimen can be fixed to coincide with the predicted in-situ sliding direction if the specimen is oriented and so marked prior to its removal from the rock exposure or outcrop. Regardless of whether the specimen is a clean joint in hard rock or a block of fault gouge, it should not be disturbed more than necessary during extrication from the outcrop and during packaging and shipping. If the natural fracture of interest separates a sample block into two pieces, they should be securely wrapped or taped to assure minimal movement along the fracture. Drill core specimens can also be used in direct shear testing of natural discontinuities. Each laboratory specimen is tested wet or dry according to expected field conditions. Shearing rates and other aspects of testing should be based on appropriate guidelines, such as those suggested by the International Society for Rock Mechanics (1974) and the Rock Testing Handbook - Test Standards (U. S. Army Engineer Waterways Experiment Station 1980).

70. The typical laboratory direct shear test is performed on two blocks of rock separated by a discontinuity. Irregularly shaped blocks are trimmed and then cast in quick-set cement in a mold properly sized for the shear box on the shearing machine. A load is applied to the blocks perpendicular to the fracture, and the shear load required to displace the blocks relative to each other is monitored (Figure 16). Fault gouge or soft rock specimens are tested in a similar fashion, but a single block of material is sheared through its intact substance.

71. Slope stability analyses often rely on residual shear strengths estimated from laboratory tests because experience has shown that these strengths generally provide good approximations of those expected in the field.* The

---

* Personal communication, J. P. Savely, Inspiration Consolidated Copper Co., Inspiration, Ariz., 1980.

Personal communication, R. D. Call, Pincock, Allen, and Holt, Inc., Tucson, Ariz., 1979.

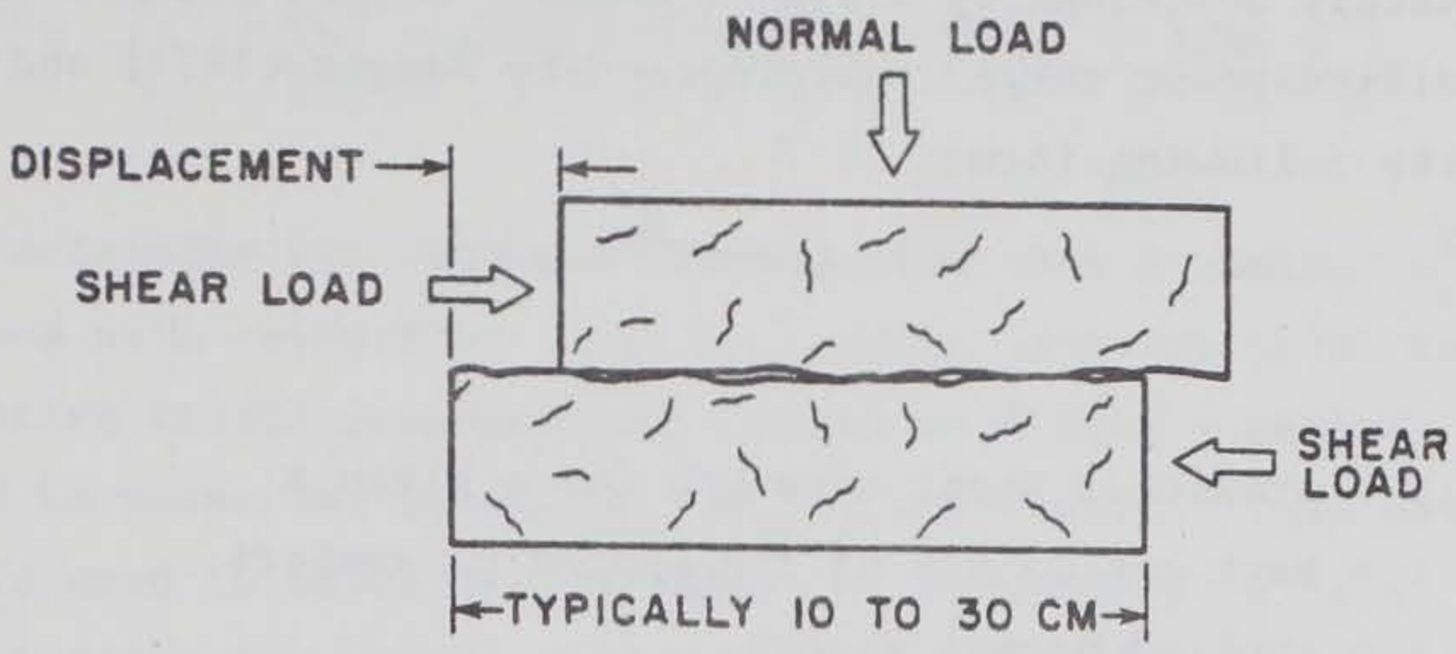

a. Loading diagram for direct shear test

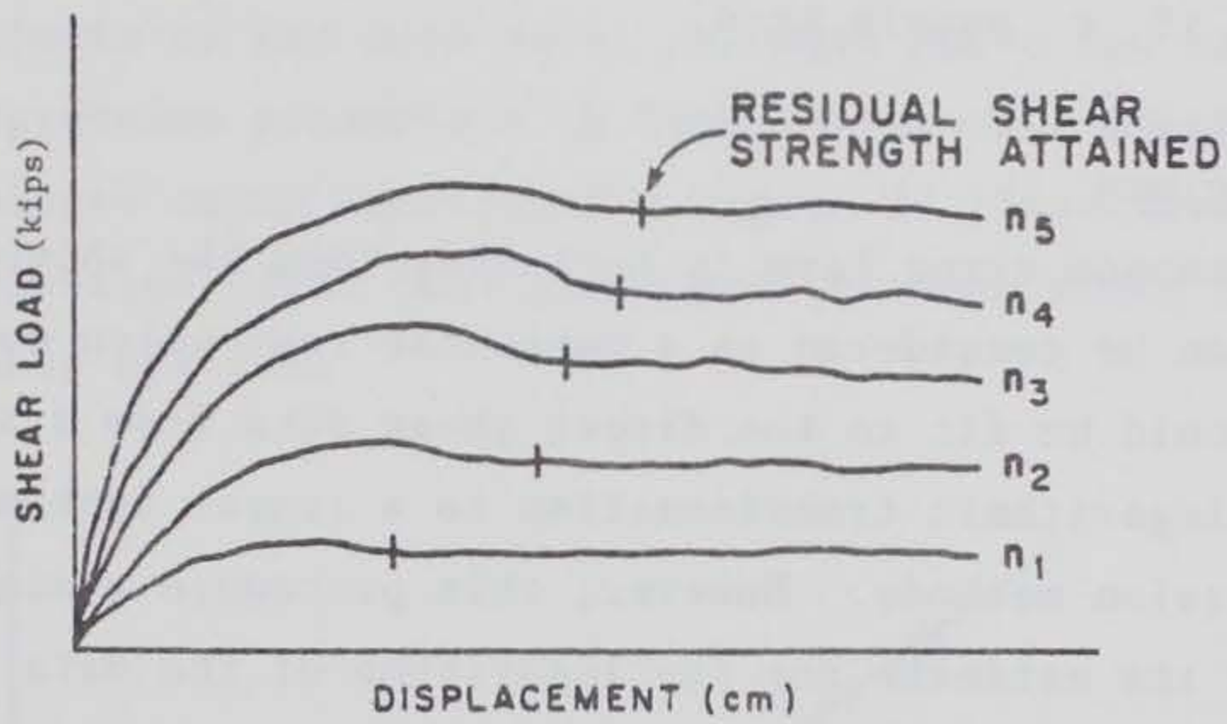

b. Laboratory test curves for five normal loads

Figure 16. Direct shear loading diagram and laboratory curves

residual shear strength of a discontinuity is attained when an increase in shear displacement is not accompanied by an increase in shear load. The displacement at each residual point is then used to calculate the corresponding contact area in shear. This area is divided into the appropriate normal and shear loads to obtain normal and shear stresses for each residual point.

Statistical Analysis of Shear Strength

72. Results from the direct shear testing of a given specimen are displayed as a graph with normal stress plotted as the independent variable and shear strength plotted as the dependent variable. Several different least-squares regression models can be applied to these test data, the most common probably being a linear model. However, certainly not all direct shear data

can be adequately described by a linear model. A more general shear strength model (a modified power curve) was proposed by Jaeger (1971) and can be expressed in the following form:

$$y = ax^b + c \tag{6}$$

where

y = predicted shear strength for a given x

a, b, c = best estimators of regression parameters

x = applied normal stress

This nonlinear model readily degenerates to a linear form if b equals 1 or to a power curve if c equals zero.

Regression analysis
for a single specimen

73. If a random error term is included, then the above general shear strength model can be considered as a nonlinear regression model. This regression model could be fit to the direct shear data from a single test specimen by making a logarithmic transformation to a linear system and then applying linear regression methods. However, this procedure minimizes the mean squared error of the estimate for the logarithms of the data values, not for the data values themselves.

74. A numerical approximation method can be used to obtain a modified power curve fit that directly minimizes the mean squared error of the estimate of the dependent variable (shear strength) for a particular test specimen. This expected squared error of the estimate is given by:

$$s_e^2 = \frac{1}{N - 3} \sum_{n=1}^{N} \left(y_n - ax_n^b - c \right)^2 \tag{7}$$

where

s_e^2 = expected squared error of the estimate

N = total number of data points

y_n = shear strength of the n^{th} data point

x_n = normal stress of the n^{th} data point

After expanding the square and implementing some algebra, Equation 7 can be rewritten in the following form:

$$s_e^2 = \frac{1}{N - 3} \left(c^2 + \sum_n y_n^2 + a^2 \sum_n x_n^{2b} + 2ac \sum_n x_n^b - 2c \sum_n y_n - 2a \sum_n y_n x_n^b \right) \quad (8)$$

75. To determine the regression parameters that minimize s_e^2 the partial derivatives with respect to a, b, and c are set equal to zero. Then, an iterative calculation procedure based on Newton's method of approximation is used to solve for parameter b (Miller 1982c). This estimated value of b is used to calculate estimates of parameters a and c. All of these calculations can be easily programmed on any desktop computer.

76. Consequently, for the particular test specimen under study the least-squares estimate of the mean shear strength curve can be defined using the calculated regression parameters in Equation 6. The squared error of the estimate is calculated using Equation 7. Figure 17 illustrates the nonlinear, least-squares regression curve that describes the mean shear strength of a typical direct shear specimen.

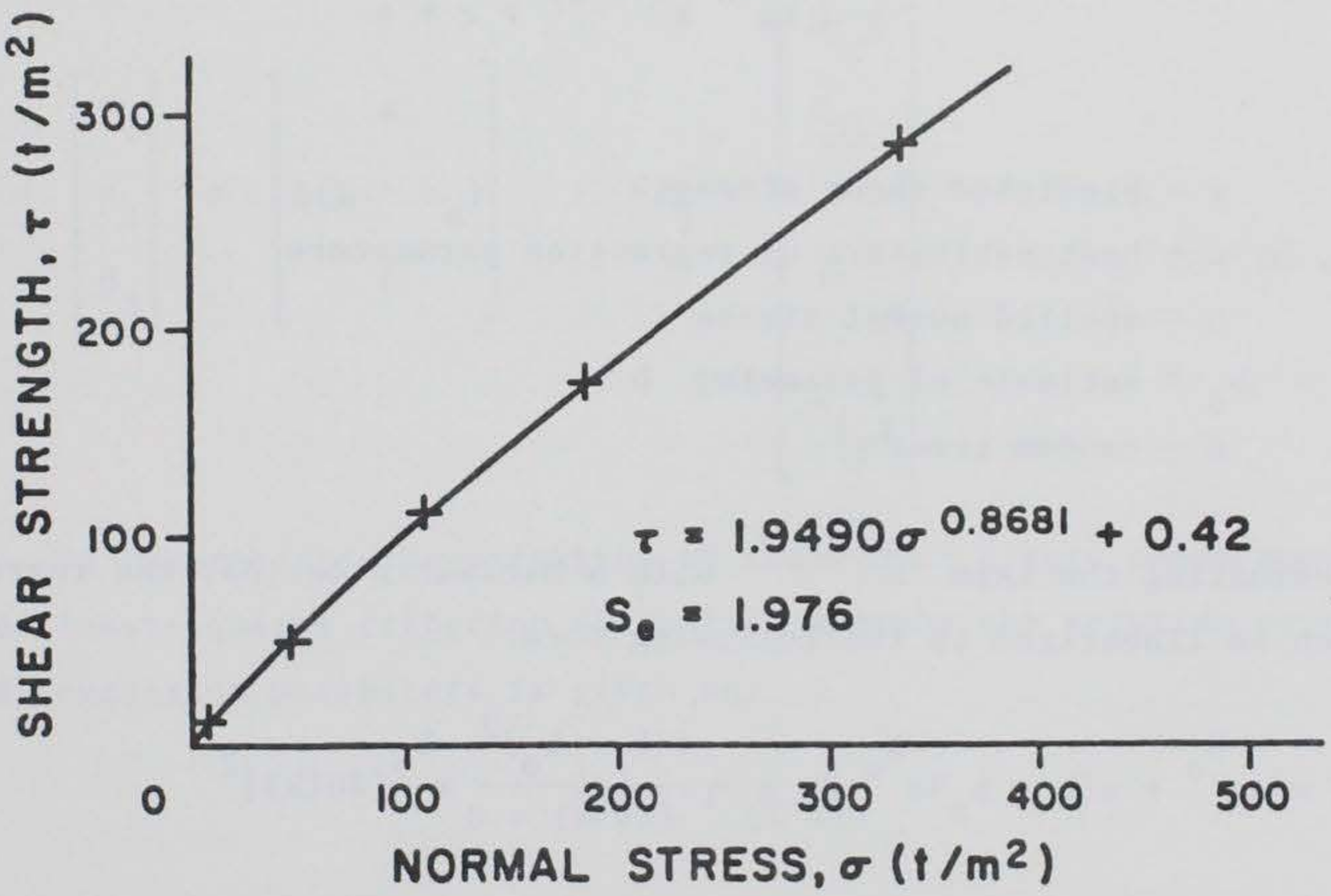

Figure 17. Nonlinear regression curve describing the shear strength of a natural joint in oil shale

Weighted regression analysis
for a group of like specimens

77. A probabilistic slope stability analysis cannot be based on the results of a single direct shear test. Commonly, four or more specimens that

contain a given type of discontinuity are tested to provide a data set suitable for estimating the shear strength along that particular type of geologic discontinuity. Strength estimates obtained from these similar specimens should be statistically combined to determine the distribution of shear strengths for that particular group or population. In essence, several regression curves must be combined to produce a regression curve representative of the population. Curves from some of the specimens provide better estimates of the population curve than others. Therefore, a weighted regression scheme is desirable for combining the curves.

78. A modified power curve regression model can be linearized by approximating the power term with a Maclaurin series (Draper and Smith 1981). An iterative calculation procedure is then used to solve for the three regression parameters. The nonlinear regression model can be expressed in the following form:

$$y = ax^{b_o} x^{(b-b_o)} + c + \varepsilon \tag{9}$$

where

y = predicted shear strength

a, b, c = best estimators of regression parameters

x = applied normal stress

b_o = estimate of parameter b

ε = random error

By approximating the term $x^{(b-b_o)}$ with a Maclaurin series, the regression model can be linearized to the following form:

$$y = ax^{b_o} + a(b - b_o)x^{b_o} \ell n\, x + \frac{a(b - b_o)^2}{2} x^{b_o}[\ell n(x)]^2 + \frac{a(b - b_o)^3}{3!} x\, b_o(\ell n\, x)^3 + \ldots + c + \varepsilon \tag{10}$$

79. Experience has shown that the use of only the first two terms in the series expansion provides good estimates of the regression parameters; whereas, the use of additional terms often produces a curve with unreasonable fluctuations and overall poor estimation of y (Miller 1982c). For combining

the test results of like specimens, let J be the number of specimens and I_j be the number of data points for the j^{th} specimen. Then, a suitable approximation of Equation 10 can be written in the following matrix notation:

$$Y_j = X_j \beta + \varepsilon_j \tag{11}$$

where

$$Y_j = \begin{bmatrix} y_{1j} \\ y_{2j} \\ \cdot \\ \cdot \\ \cdot \\ y_{I_j J} \end{bmatrix} \qquad X_j = \begin{bmatrix} b_o & b_o & \\ x_{1j} & x_{1j} \ln(x_{1j}) & 1 \\ b_o & b_o & \\ x_{2j} & x_{2j} \ln(x_{2j}) & 1 \\ \cdot & \cdot & \cdot \\ \cdot & \cdot & \cdot \\ \cdot & \cdot & \cdot \\ b_o & b_o & \\ x_{I_j J} & x_{I_j J} \ln(x_{I_j J}) & 1 \end{bmatrix}$$

$$\beta = \begin{bmatrix} \beta_1 \\ \beta_2 \\ \beta_3 \end{bmatrix} = \begin{bmatrix} a \\ a(b - b_o) \\ c \end{bmatrix} \qquad \varepsilon_j = \begin{bmatrix} \varepsilon_{1j} \\ \varepsilon_{2j} \\ \cdot \\ \cdot \\ \cdot \\ \varepsilon_{I_j J} \end{bmatrix}$$

80. To incorporate the weighting of individual direct shear specimens, a weighted least-squares criterion is applied whereby the solution vector of estimated regression parameters is given as:

$$\hat{\beta} = (X'WX)^{-1} (X'WY) \tag{12}$$

where

$$X'WX = \sum_{j=1}^{J} X_j' W_j X_j$$

$$X'WY = \sum_{j=1}^{J} X_j' W_j Y_j$$

81. Diagonal elements in a given W_j matrix can be arbitrarily assigned, but are usually set equal to the inverse of the standard error from the regression of the j^{th} specimen (s_{e_j}), the assumption being that greater confidence can be placed in the reliability of a regression curve with a smaller standard error. The weight matrix for the j^{th} specimen has dimensions I_j by I_j and is typically given as:

$$W_j = \begin{bmatrix} w_j & 0 & 0 & 0 \\ 0 & w_j & 0 & 0 \\ 0 & 0 & w_j & 0 \\ & & & \ddots \\ 0 & 0 & 0 & w_j \end{bmatrix} = \begin{bmatrix} 1/s_{e_j} & 0 & 0 & 0 \\ 0 & 1/s_{e_j} & 0 & 0 \\ 0 & 0 & 1/s_{e_j} & 0 \\ & & & \ddots \\ 0 & 0 & 0 & 1/s_{e_j} \end{bmatrix} \qquad (13)$$

82. Equation 12 can be solved provided that the X'WX matrix has an inverse. The numbers of data points can even vary from one specimen to another, because the X'WX matrix will always be dimensioned 3 by 3 and the X'WY matrix will always be dimensioned 3 by 1.

83. Iterative calculations to determine the solution vector begin with the application of Newton's approximation method to a set of interpolated data points. (This set usually consists of 30 to 50 points.) Each of these points has a normal stress value x_o between zero and the maximum normal stress used in testing. Each has a shear strength value equal to the mean of the values predicted at x_o by the regression curves of the individual specimens. The results of Newton's approximation provide initial estimates of a, b, and c. The initial estimate of b is assigned to b_o, and the X_j and Y_j matrices are formed according to the expressions given directly after Equation 11. The W_j matrices are formed according to Equation 13. The solution vector $\hat{\beta}$ is obtained using Equation 12.

84. A new estimate of b is determined by the following expression:

$$b = \frac{\hat{\beta}_2}{\hat{\beta}_1} + b_o \tag{14}$$

This new estimate is assigned to b_o and the above procedures repeated until the difference between b_o and b is negligible, such as less than 0.0001. Parameters a and c for the group regression curve are respectively equal to $\hat{\beta}_1$ and $\hat{\beta}_3$ as predicted by the last iteration. Typically, less than eight iterations are required to produce the final estimates of a, b, and c for the regression curve that describes the expected shear strength of the specified discontinuity type. The estimated shear strength, $\hat{y}_o$, that corresponds to a given normal stress, x_o, is then defined by the following equation:

$$\hat{y}_o = ax_o^b + c \tag{15}$$

85. A statistical description for the expected shear strength at any given normal stress must also include the variance and the probability density function. An assumption of normality for the random errors, and thus for the expected shear strengths, is not acceptable because it would allow negative values of shear strength at small normal stress values. Consequently, at low normal stresses the probability density of shear strength is expected to favor a gamma or lognormal type of distribution. A gamma probability density function has been used by Miller (1982c) because it allows only positive shear strengths and because it closely approximates a normal density when the coefficient of variation is less than one-tenth (0.10).

86. The variance of the expected shear strength at any given normal stress, x_o, can also be directly calculated as part of the weighted, nonlinear regression analysis for a group of like specimens. The following relationship, which is partially based on the weight matrix defined in Equation 13, has been developed to determine this variance (Miller 1982c):

$$\mathrm{Var}(\hat{y}_o) = \underline{x}_o' \, (X'WX)^{-1} X'X (X'WX)^{-1} \underline{x}_o \tag{16}$$

where

$$X'WX = \sum_{j=1}^{J} X_j' W_j X_j$$

$$X'X = \sum_{j=1}^{J} X_j' X_j$$

$$\underline{x}_o = \begin{bmatrix} x_o^b \\ x_o^b \ln(x_o) \\ 1 \end{bmatrix}$$

87. Figure 18 is an example graph of a weighted, nonlinear regression curve that statistically describes the shear strength of a group of four direct shear specimens of the same type. The dashed curves represent a one-standard-deviation belt about the mean curve. This type of regression analysis provides the necessary shear strength information for a probabilistic slope stability analysis. Regardless of which type of probability density function is used to describe the shear strength, its parameters are defined by

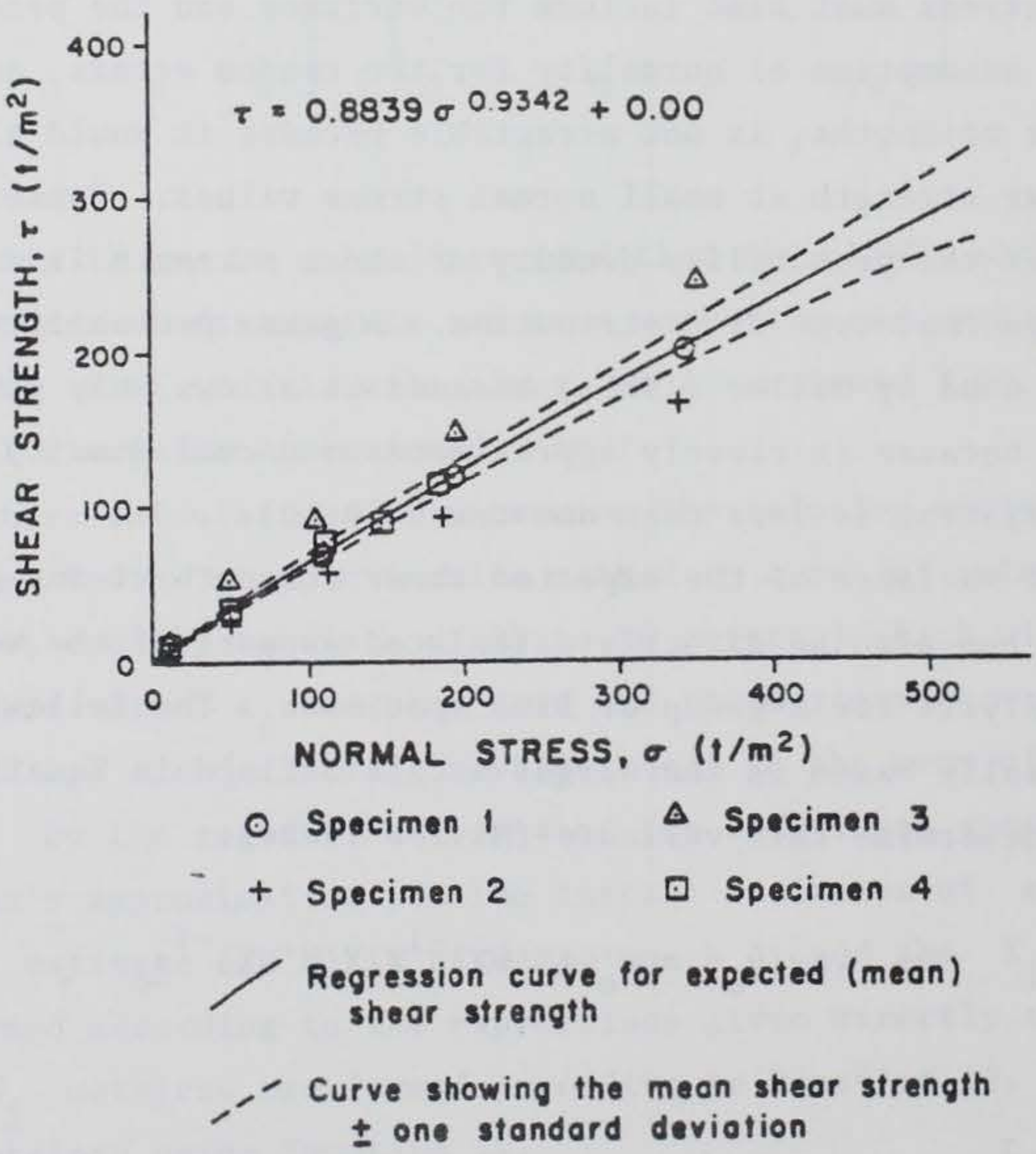

Figure 18. Weighted, nonlinear regression curve describing the shear strength of four similar direct shear specimens

the mean and variance of the shear strength at any specified normal stress. Therefore, once a normal stress has been calculated in a stability analysis, the probability distribution of the corresponding shear strength can be readily determined.

Summary

88. Representative rock strength parameters can be obtained by laboratory tests that estimate rock substance strength and discontinuity shear strength. Some of the parameters are required input for rock slope stability analyses, while others are important for the comparison and classification of rock types within a study area and among different study areas.

89. Results of a rock strength testing program can be succinctly summarized by rock type to help in subsequent engineering evaluations and analyses. An example of a tabulated rock strength summary for the quartz latite porphyry (QLP) shown in Figure 15 is given below in Table 2.

Table 2

Example Rock* Strength Summary for QLP

	No.	Mean	Standard Derivation	Minimum	Maximum
Unconfined compressive strength, psi**	4	13,554	2,110	11,120	16,982
Triaxial compressive results:					
Cohesion, psi	4	1,003	--	--	--
Coefficient of Friction	4	1.122	--	--	--
Brazilian tensile strength, psi	6	1,568	401	1,157	2,035
Density, pcf†	12	171.6	7.9	163.7	181.8
RQD, percent	37	82.3	9.2	54.3	99.5
Clean joint shear strength:	5				
(regression model: $\tau = 1.696\sigma^{0.836} + 0.24$)					
τ, psi for σ = 10 psi		11.9	1.7	--	--
σ = 50 psi		44.8	2.1	--	--
σ = 200 psi		142.5	6.4	--	--
σ = 400 psi		254.2	14.2	--	--

* Rock Substance Classification: Medium to high compressive strength with a medium modulus ratio.

** To convert pounds per square inch (psi) to pascals, multiply by 6894.747.

† To convert pounds per cubic foot (pcf) to kilograms per cubic metre, multiply by 16.01846.

PART V: PROBABILISTIC STABILITY ANALYSES FOR COMMON FAILURE MODES

90. For any slope cut in a discontinuous rock mass characterized by multiple fracture orientations, predicting the exact failure geometry is exceedingly difficult, if not impossible. Therefore, simplified instability models and statistical estimates of fracture properties and shear strengths are used to provide probabilistic estimates of slope stability. The instability models are considered as potential failure modes and are studied with either two-dimensional or three-dimensional analyses.

Identification of Failure Modes

91. Typical rock slope failure modes are illustrated in Figure 19. A brief discussion of each failure mode is given below.

92. The plane shear mode is characterized by a potential failure mass capable of sliding along a geologic discontinuity that strikes parallel or nearly parallel to the slope face and dips flatter than the slope face angle. In a two-dimensional plane shear analysis the potential sliding mass is assumed to be laterally unconstrained. This is also known as the "side-release" assumption.

93. In many rock slopes a single discontinuity often lacks the required continuous length for failure; whereas, a more complex failure path comprised of multiple fractures is likely to provide the continuous path needed for sliding. From a two-dimensional standpoint the most likely situation in practice is that two fracture sets form a stepped geometry. Both sets strike parallel or nearly parallel to the strike of the slope, and sliding occurs on the flatter dipping set with either separation along the steeper dipping set or tensile failure of intact rock bridges that connect the sliding surfaces of the flatter dipping fractures.

94. The simple wedge geometry is formed by two geologic structures that strike across the slope crest and intersect within the slope to form a tetrahedral rock prism. Sliding will occur along the line of intersection, which implies that for a wedge to be kinematically viable its intersection line must be daylighted by the slope face. Three-dimensional vectorial methods are available for analyzing the stability of simple, rigid-block wedges (Wittke 1965, and Goodman and Taylor 1967) and are preferred over stereographic

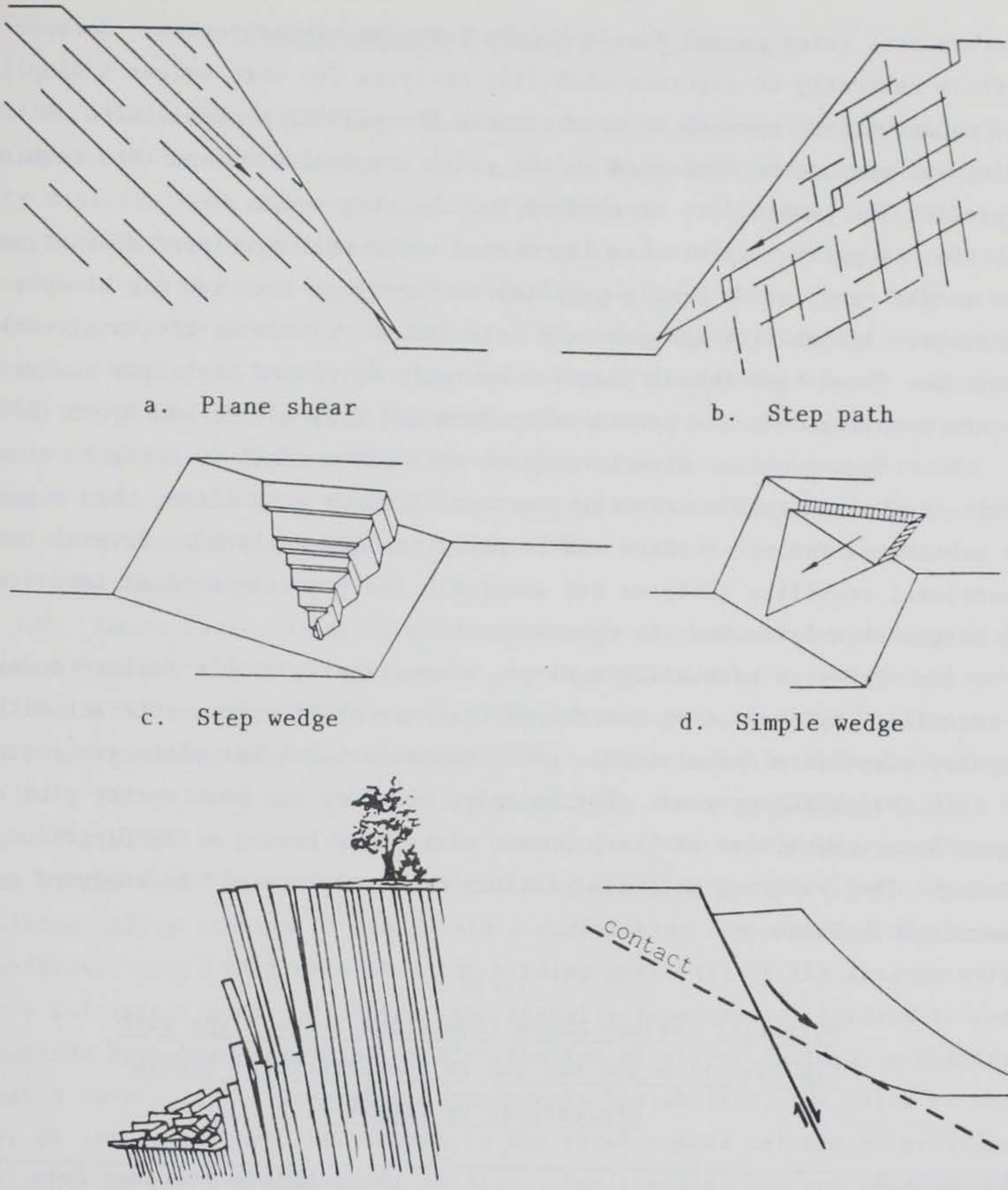

a. Plane shear

b. Step path

c. Step wedge

d. Simple wedge

e. Toppling

f. General surface

Figure 19. Typical failure modes for rock slopes

projection methods for purposes of computer compatibility and calculation efficiency.

95. The step-wedge failure mode is similar to the simple wedge, except the structures that intersect to form the geometry of the step wedge are not single planar structures. Rather, it is assumed that combinations of different

fracture sets (step paths) form a highly irregular intersection. Because there is currently no rigorous stability analysis for step wedges a simplistic, conservative approach is used whereby the sliding probabilities of the individual step paths contained in the wedge are evaluated and then combined to predict the probability of sliding for the step wedge.

96. Toppling failure usually occurs where well developed discontinuities strike parallel or nearly parallel to the slope face and dip steeply into the slope. Instability involves the rotation of columns or blocks of rock about some fixed base (basal plane). Recently developed stability analyses for the toppling mode are presented by Hoek and Bray (1977) and Brown (1982).

97. When a unique structure (such as a major fault or contact) or a combination of definable structures occurs within a rock slope, then a general (or arbitrary) failure surface can be predicted and analyzed. Several two-dimensional stability analyses are available for general surfaces including the Morgenstern-Price and the Spencer methods.

98. Prior to excavating a slope, kinematically viable failure modes can be identified by evaluating how mapped fracture orientations interact with the proposed slope face orientation. Lower-hemisphere Schmidt plots are essential for this evaluation process. For example, consider the mean vector plot of Figure 8 in conjunction with a proposed slope face having a dip direction of 330 deg. The resulting potential failure modes that should be analyzed are summarized in Table 3.

Table 3

Potential Failure Modes Identified for a Slope with Dip Direction 330 deg Cut in the Structural Domain Represented by Figure 8

Failure Mode	Responsible Fracture Sets
Plane shear	30.2, 32.5
Step path	30.2/32.5, 30.2/14.8, 32.5/14.8
Simple wedge	0.4/29.5, 0.4/28.8, 0.4/26.5, 1.6/29.5, 1.6/28.8
Step wedge	0.4/1.6 with 29.5/28.8
Toppling	14.8

Estimating the Probability of Sliding

99. For a specified slope geometry and failure mode the probability of sliding can be estimated using basic equilibrium considerations and the probability distributions of pertinent input parameters. A popular index for evaluating stability of a potential failure mass is the factor of safety, which is the ratio of total force that resists sliding to total force that induces sliding (Hoek and Bray 1977). A condition of limiting equilibrium is represented by a safety factor of 1.0 (resisting force equal to sliding force). If one or more of the parameters used to determine the safety factor can be considered random variables, then the safety factor must also be considered a random variable. Its probability distribution can be estimated by Monte Carlo simulation or by numerical convolution performed by discrete Fourier analysis.

Monte Carlo simulation

100. Monte Carlo simulation is a procedure to combine probability distributions of random variables to predict the distribution of a new random variable, where the new variable is a function of the other variables. The philosophy and practice of Monte Carlo methods are discussed by Newendorp (1975).

101. To estimate the probability of sliding for a particular failure mode, a distribution of safety factors is simulated by repeatedly sampling values of the input variables and calculating a safety factor. Each of the calculated safety factors is one possible realization (or outcome) of the probabilistic model that describes the sliding potential of the failure mass. After a sufficient number of iterations (usually from several hundred to over a thousand) have been completed, a distribution of safety factors is obtained. Because a safety factor less than 1 represents instability, the ratio of the number of safety factors less than 1 to the total number calculated provides an estimate of the probability of sliding. For example, 220 out of 1000 calculated safety factors are less than 1.0; thus, the probability of sliding is 0.22, or 22 percent. When the simulated safety factor distribution approximates a known probability density function, then the probability of sliding equals the area under the function where values of the safety factor are less than 1.

102. Any failure mode with a sliding potential that can be expressed in terms of a safety factor equation can be analyzed by Monte Carlo simulation. Plane-shear, step-path, and simple-wedge failure modes are in this category.

One example of a probabilistic plane shear analysis based on Monte Carlo techniques is given by Marek and Savely (1978). In addition, fairly complex "slice-analysis" methods such as the modified Bishop's method for rotational shear and Spencer's method for general surfaces can be fitted with Monte Carlo "overlays" that allow for repeated samplings and calculations that yield a distribution of possible safety factors.

103. A given Monte Carlo simulation provides only one realization of the true probability distribution of the safety factor. Another simulation, identical except for the random starting seed, will produce a slightly (or sometimes drastically) different realization. Consequently, a large number of iterations (a thousand or more) may often be required to provide consistent, stable results and a reasonable estimate of the probability of sliding. These large simulations require considerable computer time, making the associated costs objectionable and sometimes prohibitive. Fewer iterations are therefore used, resulting in a poorer estimate of the probability of sliding.

Convolution by Fourier analysis

104. Fourier analysis provides a viable alternative to Monte Carlo simulation for predicting the probability distribution of the safety factor. The probability density function (pdf) for the sum of two or more independent density functions can be expressed as the convolution of the functions with each other (Feller 1966). This implies that the sum of independent probability densities can be determined by taking the product of their Fourier transforms. An example of applying this principle in an engineering analysis is presented by Borgman (1977).

105. An efficient method for estimating the true pdf of the safety factor can be based on discrete Fourier procedures, which take advantage of the computational speed of the fast Fourier transform (FFT) algorithm. The only requirement is that the safety factor be expressed as the sum of independent random variables. Consider the plane shear failure mode shown in Figure 20. A two-dimensional stability analysis that includes the effect of waviness of the sliding surface can be based on the following safety factor equations:

$$S = \frac{\tau L + W \cos \alpha \tan R}{W \sin \alpha} \tag{17}$$

$$S = \frac{2L \sin \delta}{h^2 \sin (\delta - \alpha)} \left(\frac{\tau}{\gamma}\right) + \cot \alpha \tan R \tag{18}$$

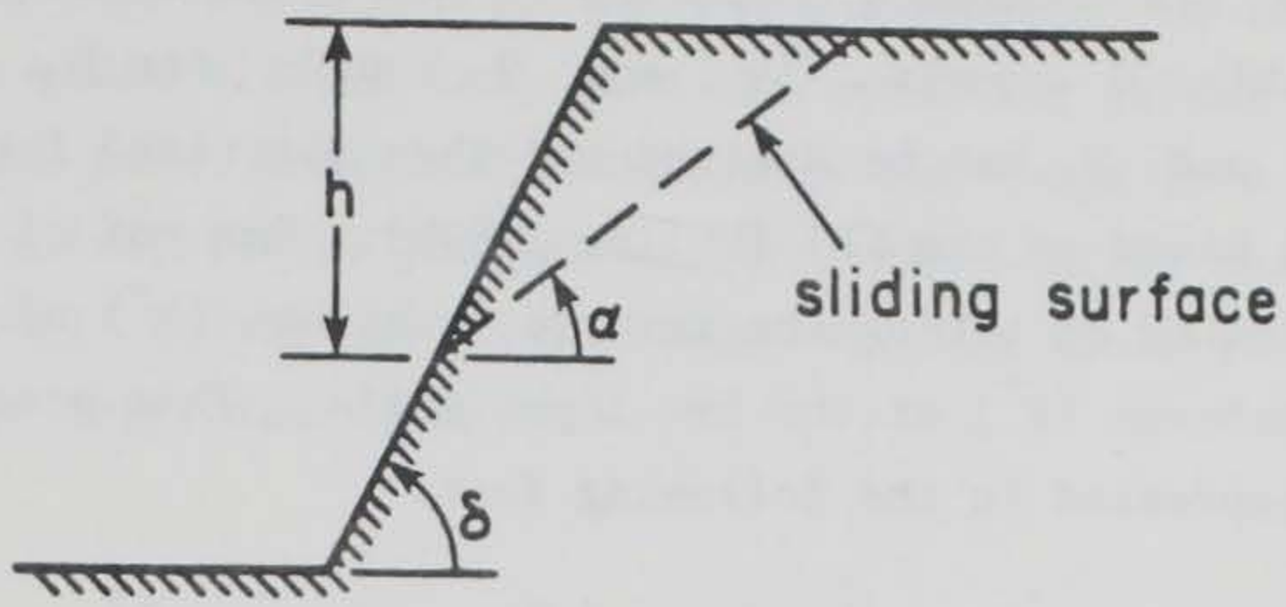

Figure 20. Rock slope with typical plane-shear failure mode

where

S = safety factor

L = length of sliding surface

W = weight of potential failure mass

α = average dip of sliding surface

R = estimated waviness of the sliding surface

δ = average dip of slope face

h = height of potential failure mass

τ = estimated shear strength along sliding surface (depends on the calculated effective normal stress which includes pore-water pressure)

γ = estimated rock density

106. For a specified slope geometry and sliding surface all the parameters are assumed constant except for the shear strength, waviness, and rock density, which are random variables with probability densities approximated by either laboratory testing data or fracture mapping data. The shear strength pdf is given by the weighted, nonlinear regression analysis of direct shear test results and is assumed to be a gamma pdf. The waviness is commonly assumed to be exponentially distributed and is estimated from fracture mapping data. The rock density is estimated from laboratory tests and is usually considered to be normally distributed. Often the rock density can be assumed constant because it has such a small coefficient of variation, typically less than 0.08. This coefficient equals the standard deviation divided by the mean.

107. Equation 18 can be expressed in the form:

$$S = AU + BV \tag{19}$$

where A and B are constants comprised of the fixed input parameters. The new random variable U equals τ/γ , and V equals tan R . The probability densities of U and V can be derived and then digitized for use in a convolution process based on the FFT (Miller 1982b). The pdf of the safety factor is then estimated by taking the reverse transform (F^-) of the product of the Fourier transforms (F^+) of the two input pdf's. This procedure can be mathematically expressed in the following form:

$$f_S(s) = F^- \left\{ F^+ \left[f_{U^*}(u^*) \right] \cdot F^+ \left[f_{V^*}(v^*) \right] \right\} \tag{20}$$

where

U^* = random variable equal to AU

V^* = random variable equal to BV

$f_{U^*}(u^*)$ = pdf of random variable U^*

$f_{V^*}(v^*)$ = pdf of random variable V^*

108. The probability of sliding is then obtained using numerical integration to calculate the area under the safety factor pdf where the safety factor has values less than 1.

109. The convolution method based on the FFT offers an improvement over Monte Carlo simulation. Most importantly, Fourier procedures provide the explicit safety factor pdf rather than a simulated realization of the pdf as produced by Monte Carlo techniques that are often prone to computational instability and excessive computer time. Preliminary comparative studies have shown that FFT convolution uses at least one-third to one-fifth the computer time required by Monte Carlo simulation using a moderate number of iterations (Miller 1982b).

110. Fourier procedures have also been developed for the step-path and simple-wedge failure modes (Miller 1982c). In the step path analysis the following three random variables must be combined: the shear strength, the waviness of the master (flatter) joint set, and the tensile strength of the rock bridges (estimated from Brazilian disc tension tests). Waviness is neglected in the wedge analysis, and the two random variables to be combined are the estimated shear strengths of the right and left planes. As with the plane-shear mode, pore-water pressure is included in these analyses via the effective normal stress that determines shear strength.

111. For all three failure modes the discrete safety factor pdf is

closely related to the input pdf of the shear strength. If the shear strength is assumed to be gamma distributed, then the resulting safety factor pdf approximates a gamma pdf. Figure 21 illustrates the comparison between a true gamma pdf and a safety factor pdf generated by the Fourier analysis of a plane-shear failure mode. The resemblance between the two tends to deteriorate as the mean waviness angle increases.

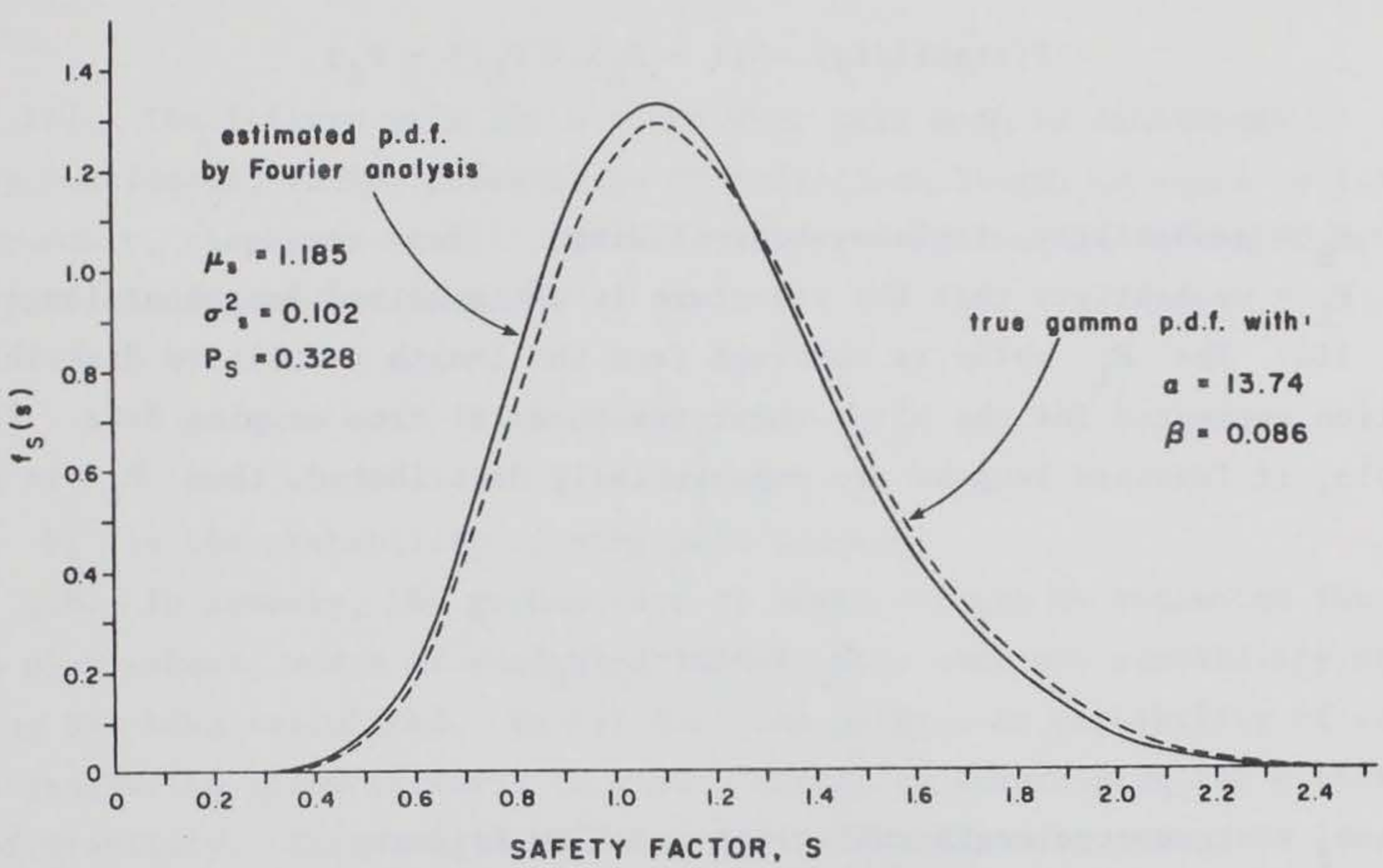

Figure 21. Comparison of a true gamma pdf with a plane-shear safety factor pdf obtained by Fourier analysis (with h = 15 m, α = 35 deg, δ = 65 deg, dry slope)

Estimating the Probability of Stability

112. Stability of a given plane-shear failure mode is a function not only of its sliding potential but also of the length of the sliding surface. To be of sufficient length for failure the sliding surface must extend continuously or nearly continuously from its daylighting point on the slope face to the upper surface (crest) of the slope.

113. Stability of a potential plane-shear failure mass is realized in one of two ways:

a. The plane-shear structure is not long enough to allow failure.

b. The plane-shear structure is long enough, but sliding does not occur.

If structure length and sliding are assumed independent, then the probability of stability is given by:

P(stability) = P(structure not long enough)
+ P(structure long enough
and no sliding occurs)

$$P(\text{stability}) = (1 - P_L) + P_L(1 - P_S) \tag{21}$$

where

P_S = probability of plane-shear sliding

P_L = probability that the structure is the required length or longer

114. The P_L value is obtained from the length cumulative distribution function estimated for the plane-shear fracture set from mapping data. For example, if fracture lengths are exponentially distributed, then P_L is given by:

$$P_L = \exp(-L_r/\mu_L) \tag{22}$$

where

L_r = structure length sufficient to allow failure

μ_L = mean fracture length for the plane-shear fracture set

115. Likewise, stability of a potential wedge failure mass is realized in one of two ways:

a. The wedge intersection is not long enough to allow failure.

b. The wedge intersection is long enough, but sliding does not occur.

If intersection length and sliding are assumed independent, then the probability of wedge sliding is given by:

P(stability) = P(intersection not long enough)
+ P(intersection long enough
and no sliding occurs)

$$P(\text{stability}) = (1 - P_{L^*}) + P_{L^*}(1 - P_S) \tag{23}$$

where

P_S = probability of wedge sliding

P_{L*} = probability that the wedge intersection is the required length or longer

116. The P_{L*} value is the joint probability that both structures comprising the wedge are long enough to allow failure (that is, $P_{L*} = P_{L_{left}} \cdot P_{L_{right}}$).

117. The failure path for a given step path mode is continuous or nearly continuous, so its probability of sufficient length is equal to 1. Consequently, step-path stability is directly related to the estimated probability of sliding and is given by:

$$P(\text{stability}) = 1 - P_S \tag{24}$$

where P_S is the probability of step-path sliding.

118. In summary, the probability of stability can be estimated for a given plane-shear, wedge or step-path failure mode once its probability of sliding has been calculated. Except for step paths, the probability of sufficient length (to allow failure) is also a factor in determining the probability of stability. This length probability is calculated by using the length cumulative distribution function of the fracture set (or sets) responsible for the failure mode.

PART VI: PROBABILISTIC SLOPE DESIGN PROCEDURES

119. The probabilistic design of a slope cut in fractured rock should include the variabilities in fracture set properties and the occurrences of multiple sliding surfaces for all failure modes present. Fracture sets that comprise the failure modes can be simulated using the statistical and spatial properties estimated from fracture mapping data. The probability of stability can then be calculated for each potential failure geometry formed by the simulated fracture sets. The individual probability values are then combined to predict the stability of the rock slope and provide useful design parameters.

Simulation of Spatially Correlated Fracture Set Properties

120. Procedures for simulating fracture set properties by Monte Carlo methods are based on random sampling of the probability distributions estimated for the properties (Marek and Savely 1978, and Call and Nicholas 1978). These methods are incapable of incorporating known spatial correlations and often require excessive amounts of computer time.

121. Spectral analysis procedures that take advantage of the computational speed of the FFT algorithm can be used to efficiently simulate spatially correlated fracture set properties. A series of simulated values generated in this way will have the desired mean, variance, and variogram function. Spatial correlation is incorporated via the digitized covariance function, which is derived from the estimated variogram function according to the following relationship (Journel 1974):

$$C(h) = \sigma^2 - \gamma(h) \tag{25}$$

where

$C(h)$ = value of covariance function at lag h

h = lag, or separation distance, between sample locations

σ^2 = variance of data

$\gamma(h)$ = Value of variogram function at lag h

122. The so-called spectral density of a random process is the Fourier transform of the covariance function (Jenkins and Watts 1968, and Borgman 1973a). In discrete form the spectral density is defined as follows:

$$S_m = \Delta h \sum_{n=0}^{N-1} C_n e^{-i2\pi mn/N} \quad (26)$$

where

S_m = m^{th} discrete value of the spectral density

Δh = digitization interval for the C_n values

N = number of digitized values of the covariance function

C_n = n^{th} digitized value of the covariance function

123. Because a covariance function is real-valued and symmetric about zero, its corresponding spectral density is real-valued and symmetric about zero (Borgman 1973a). A digital estimate of the spectral density can be readily obtained by applying the FFT to the digitized covariance function. For covariance functions of fracture set properties referenced to fracture sequence number, the digitization interval, Δh, is equal to 1. The corresponding length of record, or period, T, of the digitized covariance function is given by:

$$T = N\Delta h = N \quad (27)$$

The corresponding frequency increment, Δf, of the discrete spectral density is given by:

$$\Delta f = 1/T = 1/N \quad (28)$$

124. Fourier transformation causes correlated, stationary data in the space domain to be traded for uncorrelated, nonstationary Fourier coefficients in the frequency domain (Taheri 1980). However, the variance of each coefficient is defined by the spectral density obtained by transforming the covariance function estimated from the actual data. Therefore, the essence of simulating spatially correlated properties by spectral procedures is actually a frequency-domain simulation of uncorrelated Fourier coefficients that are assigned proper variance according to the estimated spectral density. The coefficients are then reverse Fourier transformed to provide a simulated series of fracture data values that have the desired spatial covariance.

125. The first step in simulating N uncorrelated Fourier coefficients is to generate a series of N independent, psuedo-random, normally distributed

numbers with mean zero and variance 1 (Borgman 1982). Then, the real and imaginary parts of the Fourier coefficients, A_m, for $m = 0,1,2...N/2$ are assigned the proper variances, which are given below (Borgman 1973b):

If $Am = Um - iVm$, then:

$$\mathrm{Var}(U_m) = \begin{cases} TS_m & \text{, if } m = 0 \text{ or } m = N/2 \\ TS_m/2 & \text{, otherwise} \end{cases} \tag{29}$$

$$\mathrm{Var}(V_m) = \begin{cases} 0 & \text{, if } m = 0 \text{ or } m = N/2 \\ TS_m/2 & \text{, otherwise} \end{cases} \tag{30}$$

Therefore, the simulated Fourier coefficients are given by:

$$U_m = z_1 \sqrt{\mathrm{Var}(U_m)} \tag{31}$$

$$V_m = z_2 \sqrt{\mathrm{Var}(V_m)} \tag{32}$$

where z_1 and z_2 are two of the previously simulated independent, normal (0,1) numbers. Values of the remaining coefficients, those for m between N/2 and N, are assigned according to the following conjugate symmetries (Borgman 1973b):

$$\begin{aligned} U_m &= U_{N-m} \\ V_m &= -V_{N-m} \\ V_0 &= V_{N/2} = 0 \end{aligned} \tag{33}$$

126. The series of simulated Fourier coefficients is then reverse transformed by FFT to produce a spatially correlated series of normally distributed data values with mean zero and variance equal to the variance of the original data. To complete the simulation of normally distributed fracture set properties the mean of the original data is added to each value of the mean-zero series.

127. Spectral analysis procedures for simulating spatially correlated

exponential values are also needed because some fracture set properties tend to be exponentially distributed. The simulation procedures can take advantage of the statistical property that an exponential pdf is equivalent to a chi-squared pdf with two degrees of freedom.

128. If X and Y are independent, normally distributed $(0, \sigma^2)$ random variables, then the sum of their squares gives a chi-squared variable Z (multiplied by σ^2) with two degrees of freedom; that is, Z is exponentially distributed and is expressed as:

$$Z = X^2 + Y^2 \tag{34}$$

The mean and variance of Z can be derived in terms of the variance σ^2 of X or of Y (Miller 1982c) and are, respectively, given as:

$$\mu_Z = 2\sigma^2 \tag{35}$$

$$\text{Var}(Z) = 4\sigma^4 \tag{36}$$

These results show that the variance equals the mean squared, an expected relationship because Z is exponentially distributed.

129. Also, the covariance function of the random process responsible for the distribution of Z can be expressed as follows:

$$C_Z(h) = 4C^2(h) \tag{37}$$

where

$C_Z(h)$ = value of the covariance function for Z at lag h

$C(h)$ = value of the covariance function for X or Y at lag h

The covariance function for the exponential Z is known because it is directly related to the variogram function estimated from the actual exponential fracture set data. The covariance function for either X or Y is obtained using a modified version of Equation 37:

$$C(h) = \sqrt{C_Z(h)}/2 \tag{38}$$

From Equation 35 the variance of either X or Y can be obtained as follows by using the calculated mean of the exponential fracture set property:

$$\sigma^2 = \mu_Z/2 \tag{39}$$

130. The spectral-type simulation of N exponential Z values begins by generating two sets of N independent, psuedo-random normal (0,1) numbers. Using the procedures discussed earlier, N values of spatially correlated X values and N values of spatially correlated Y values are simulated where X and Y are normal and independent; and both have mean zero, variance given by Equation 39, and covariance function given by Equation 38. The desired N values of Z are then determined as follows:

$$Z_i = X_i^2 + Y_i^2 \tag{40}$$

where i ranges from 1 to N . The simulated exponential Z values will have the correct mean and spatial covariance.

131. Example simulation results for normally and exponentially distributed fracture set properties are illustrated in Figure 22.

Probabilistic Slope Analysis for Multiple Failures

132. Occurrences of multiple sliding surfaces can be incorporated into a hybrid slope stability analysis that combines probability theory and simulation. It relies on fracture set simulations (as discussed in the previous section) to generate potential failure modes in the slope and then on probability calculations to predict slope stability. Probabilities of stability for back-failure cells on the upper surface of the slope are calculated and a graph constructed to illustrate the relationships between slope face angles and the probabilities of retaining various amounts of the slope crest.

133. Slope stability is critically dependent on fracture lengths. For plane shear and wedge failure modes fracture lengths required for failure are shorter near the crest edge, thus making failures much more likely to occur near the crest edge. Even shorter step paths near the crest edge are more likely (than longer step paths) to fail because they have lesser amounts of intact rock bridges than do longer step paths.

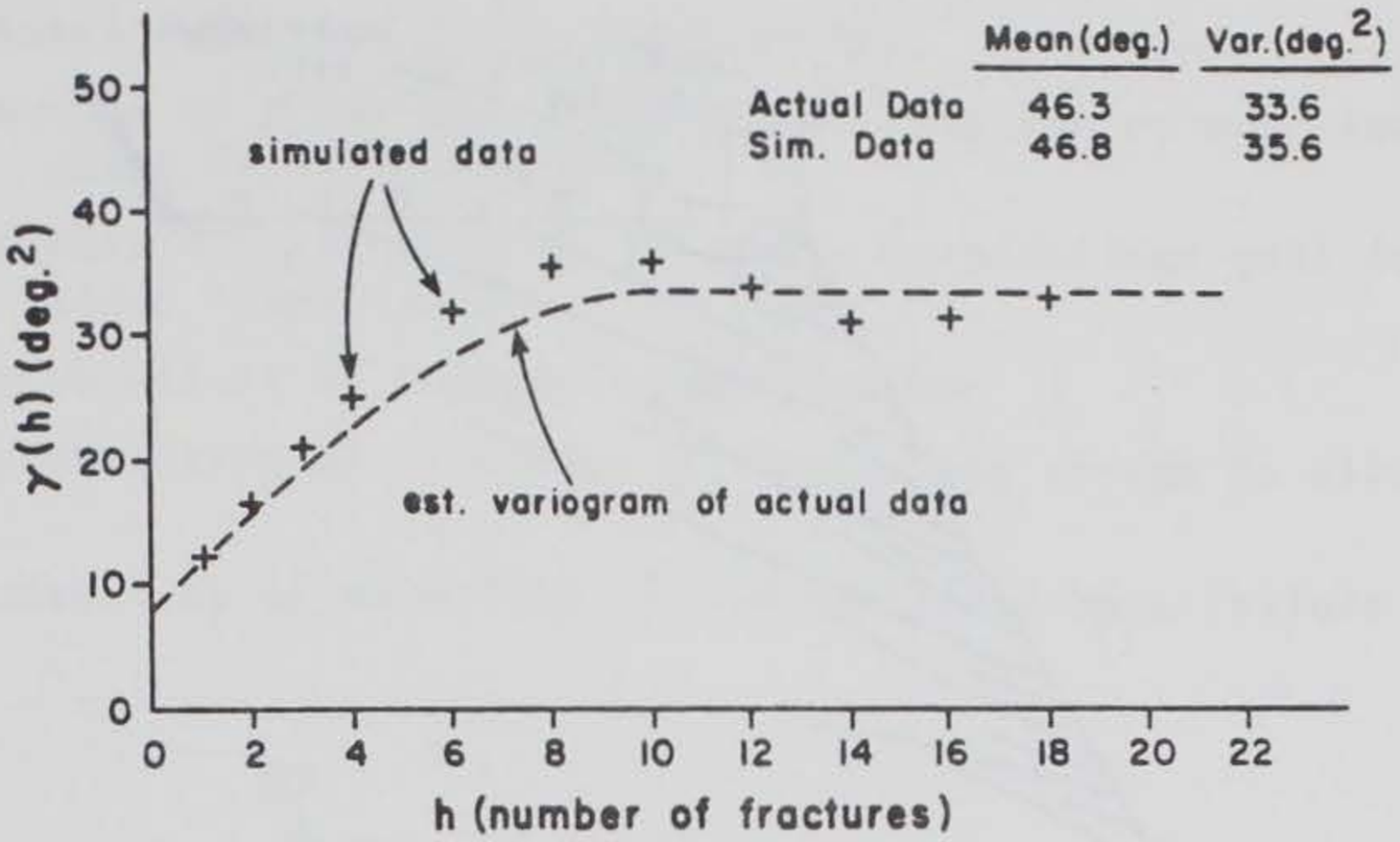

a. Results of an example simulation of fracture dips

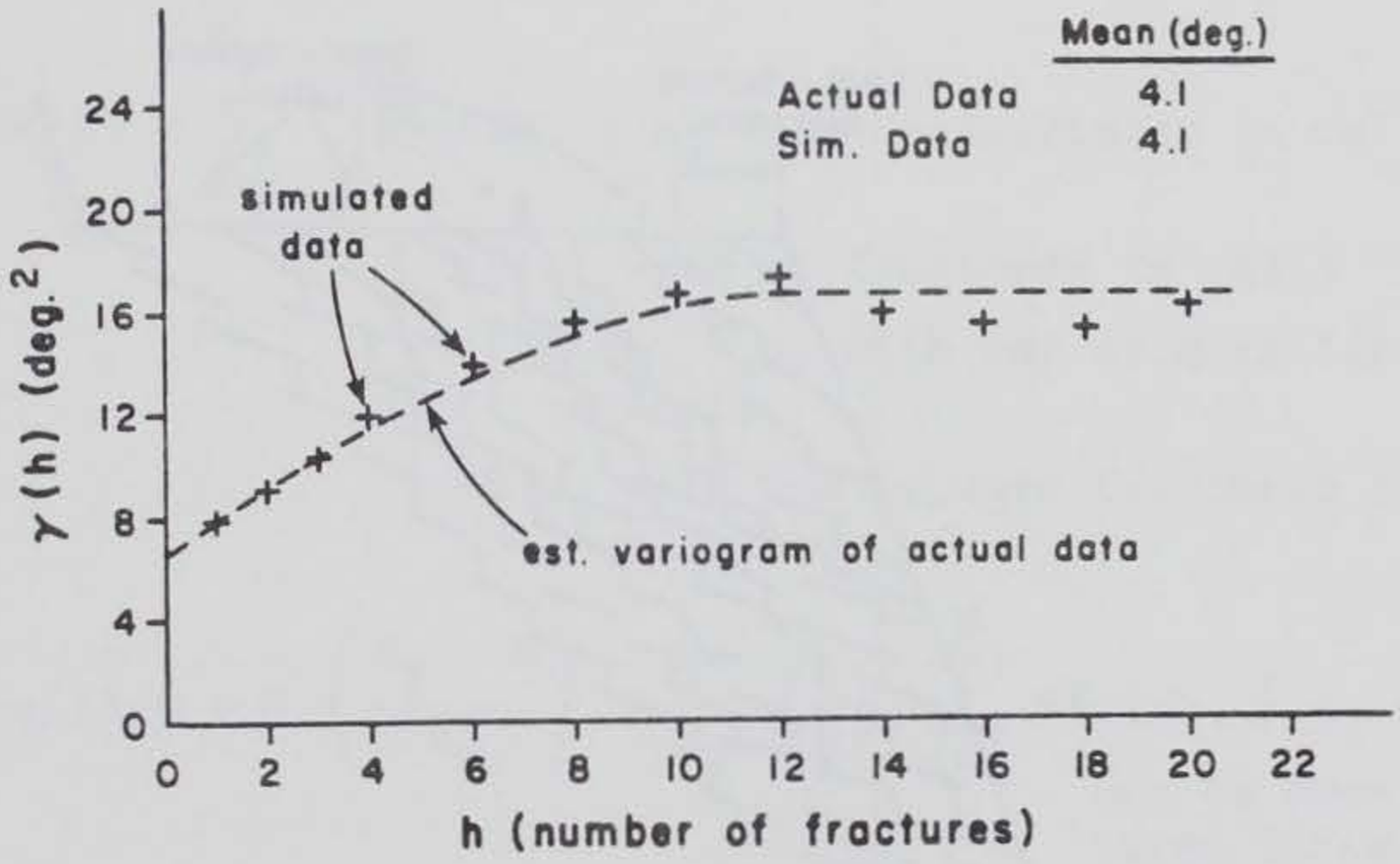

b. Results of an example simulation of fracture set waviness angles

Figure 22. Results of example simulations of 256 spatially correlated fracture set properties (Miller 1982c)

134. A typical plane shear fracture set in a slope is illustrated in Figure 23a. Back-failure distance is defined as the horizontal distance from the original edge of the slope crest back to the point where a given structure intersects the crest, or upper surface, of the slope. By simulating realizations of slopes that contain the plane-shear fracture set, the probability of stability for any given back-failure cell can be determined. Let

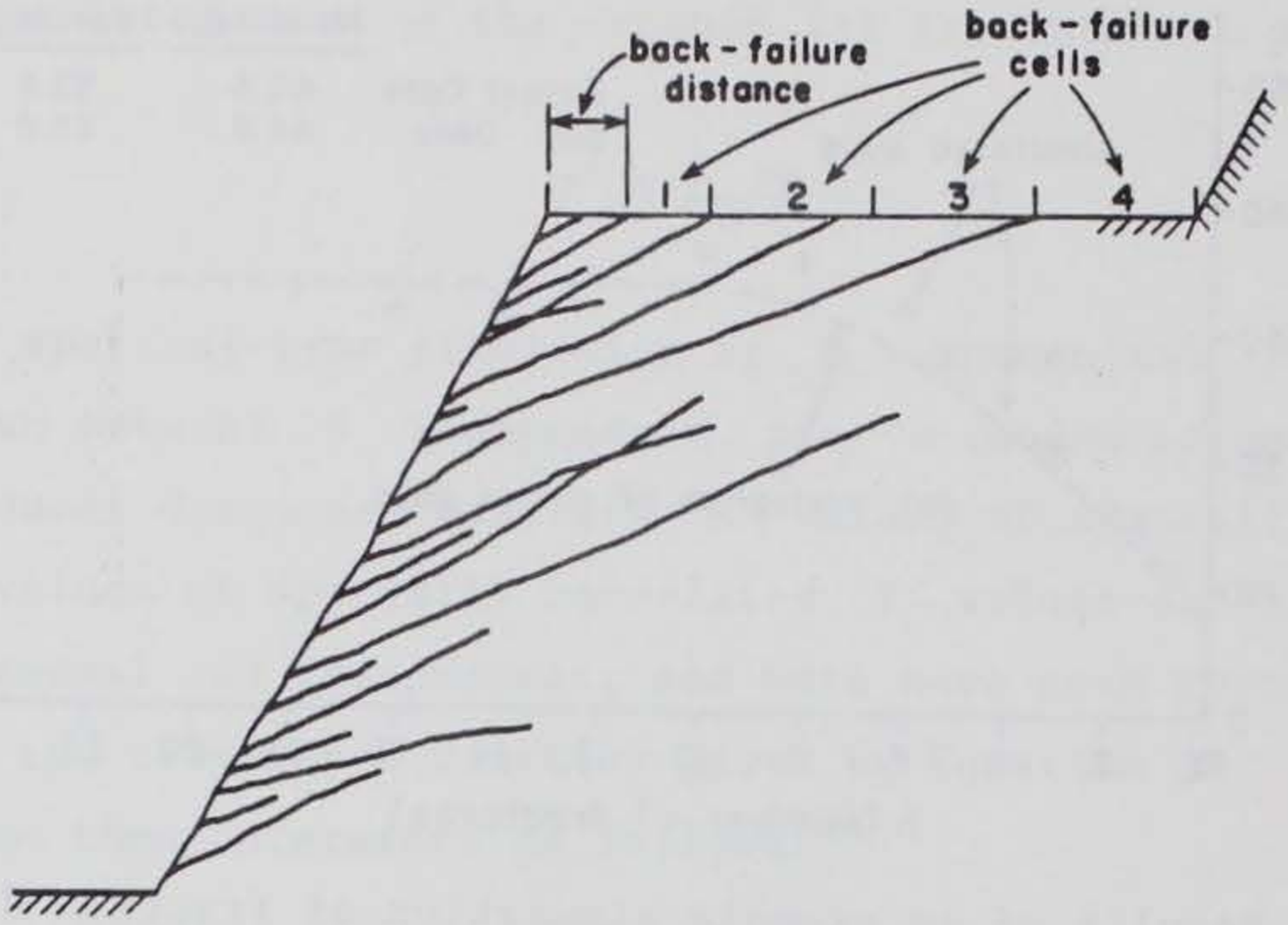

a. Plane-shear failure modes

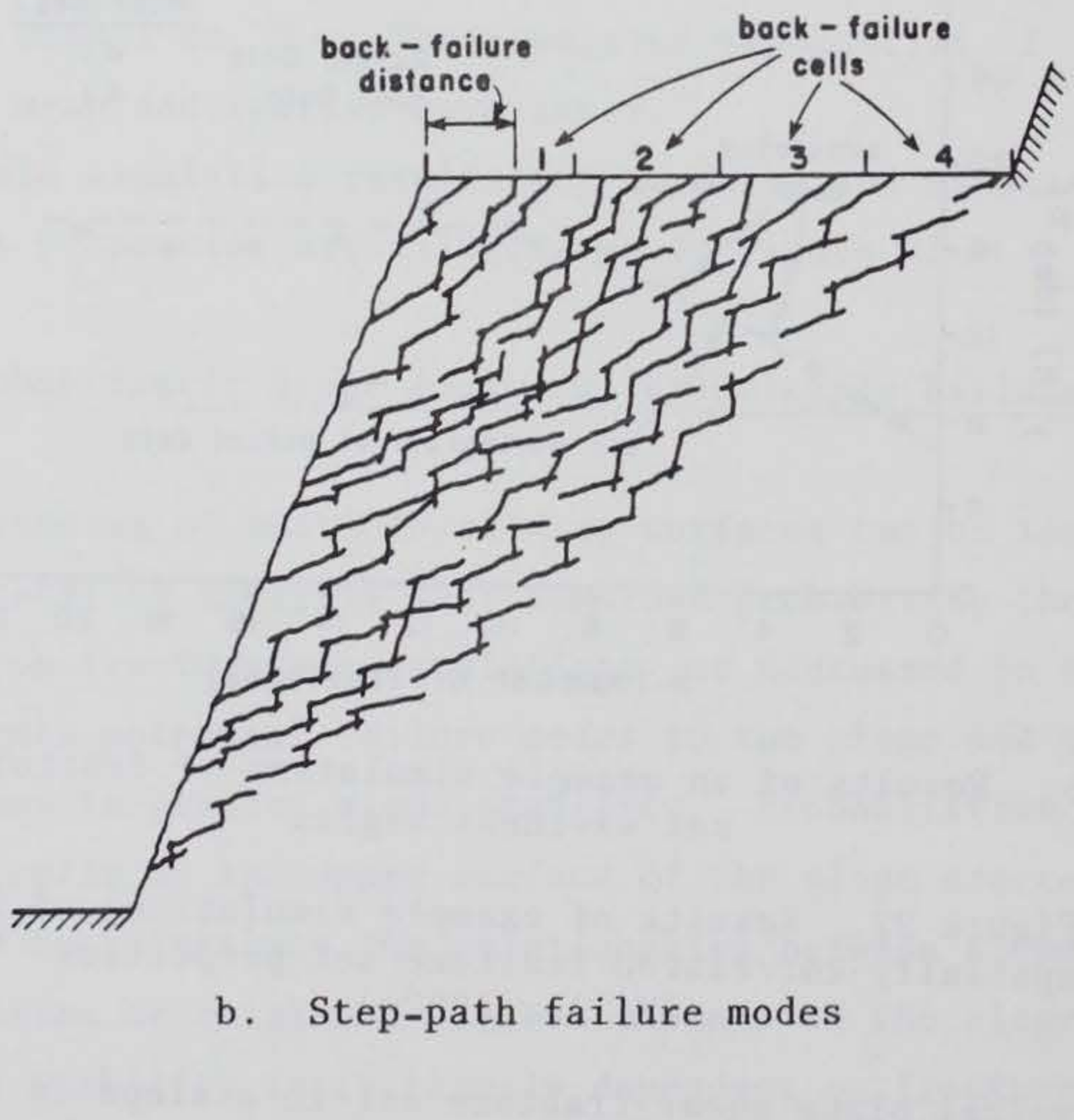

b. Step-path failure modes

Figure 23. Multiple sliding surface in a rock slope and associated back-failure cells

s_i = i^{th} slope simulation

N_T = total number of slope simulations

N = number of slope simulations that have one or more fractures in the given back-failure cell

J_i = number of fractures in the given back-failure cell for the i^{th} slope simulation

P_{S_j} = probability of sliding along fracture j

P_{L_j} = probability of fracture j being long enough to allow failure

Then, the probability of stability in the specified back-failure cell is given by:

$$P(\text{stab. in cell}) = \sum_{i=1}^{N_T} P(\text{stab.} \mid s_i \text{ with } J_i \text{ fractures in cell}) \cdot P(s_i \text{ with } J_i \text{ fractures in cell})$$

$$P(\text{stab. in cell}) = \sum_{i=1}^{N_T} \Big[P(\text{stab.} \mid s_i \text{ with no fractures in cell}) \cdot P(s_i \text{ with no fractures in cell}) + P(\text{stab.} \mid s_i \text{ with one or more fractures in cell}) \cdot P(s_i \text{ with one or more fractures in cell})\Big]$$

$$P(\text{stab. in cell}) = 1.0 \left(\frac{N_T - N}{N_T}\right) + \frac{N}{N_T}\left(\frac{1}{N}\right) \sum_{i=1}^{N} P(\text{stab.} \mid s_i \text{ with one or more fractures in cell})$$

$$P(\text{stab. in cell}) = \frac{N_T - N}{N_T} + \frac{1}{N_T} \sum_{i=1}^{N} \left\{ \prod_{j=1}^{J_i} \Big[P(\text{stab. of fracture } j \mid s_i)\Big] \right\} \tag{41}$$

$$P(\text{stab. in cell}) = \frac{N_T - N}{N_T} + \frac{1}{N_T} \sum_{i=1}^{N} \left\{ \prod_{j=1}^{J_i} \Big[(1 - P_{L_j}) \mid s_i + P_{L_j} (1 - P_{S_j}) \mid s_i\Big] \right\} \tag{42}$$

135. The probability of retaining a specified crest width is the joint probability that stability occurs in each back-failure cell contained in that width. This joint probability is mathematically expressed as follows:

$$P(\text{stab. of crest width with } N_c \text{ cells}) = \prod_{i=1}^{N_c} P(\text{stab. in cell } i) \qquad (43)$$

136. The probabilistic slope analysis begins by generating required spatially correlated properties (spacing, dip, and waviness) for the plane-shear fracture set (fractures are simulated up the slope face). Probabilities of length and sliding are computed respectively for each daylighted fracture and its associated failure mass. Probabilities of stability are then calculated and the slope simulation repeated. After the desired number of simulations (usually 4 to 8) have been completed, the crest width reliabilities can be calculated by Equations 41 and 43. The entire process is then repeated for several different slope face angles (and slope heights, if desired).

137. A slope stability graph that displays the results of a probabilistic plane shear analysis is shown in Figure 24. The information on such a graph can be combined with similar information for other failure modes present in the slope to provide useful criteria for designing the slope.

138. Step-path failure modes typically have lower probabilities of stability than plane shears of similar scale because step paths have continuous lengths except for intact rock bridges. A probabilistic analysis for multiple step paths in a slope (illustrated in Figure 23b) provides the same type of output as that for plane shears. The step-path analysis begins by generating potential step-path geometries according to a procedure from Call and Nicholas (1978) that has been modified to use spectral analysis procedures instead of Monte Carlo techniques for simulating fracture set properties. The probability of sliding is calculated for each daylighted step path. The probability of sufficient length equals 1. Probabilities of stability are then calculated and the slope simulation repeated. After the desired number of simulations (usually 6 to 12) have been completed, the crest width reliabilities can be calculated by Equations 41 and 43 with j being a counter for step paths instead of plane-shear fractures. The entire process is then repeated for several different slope face angles to produce information for a graph similar to that shown in Figure 24.

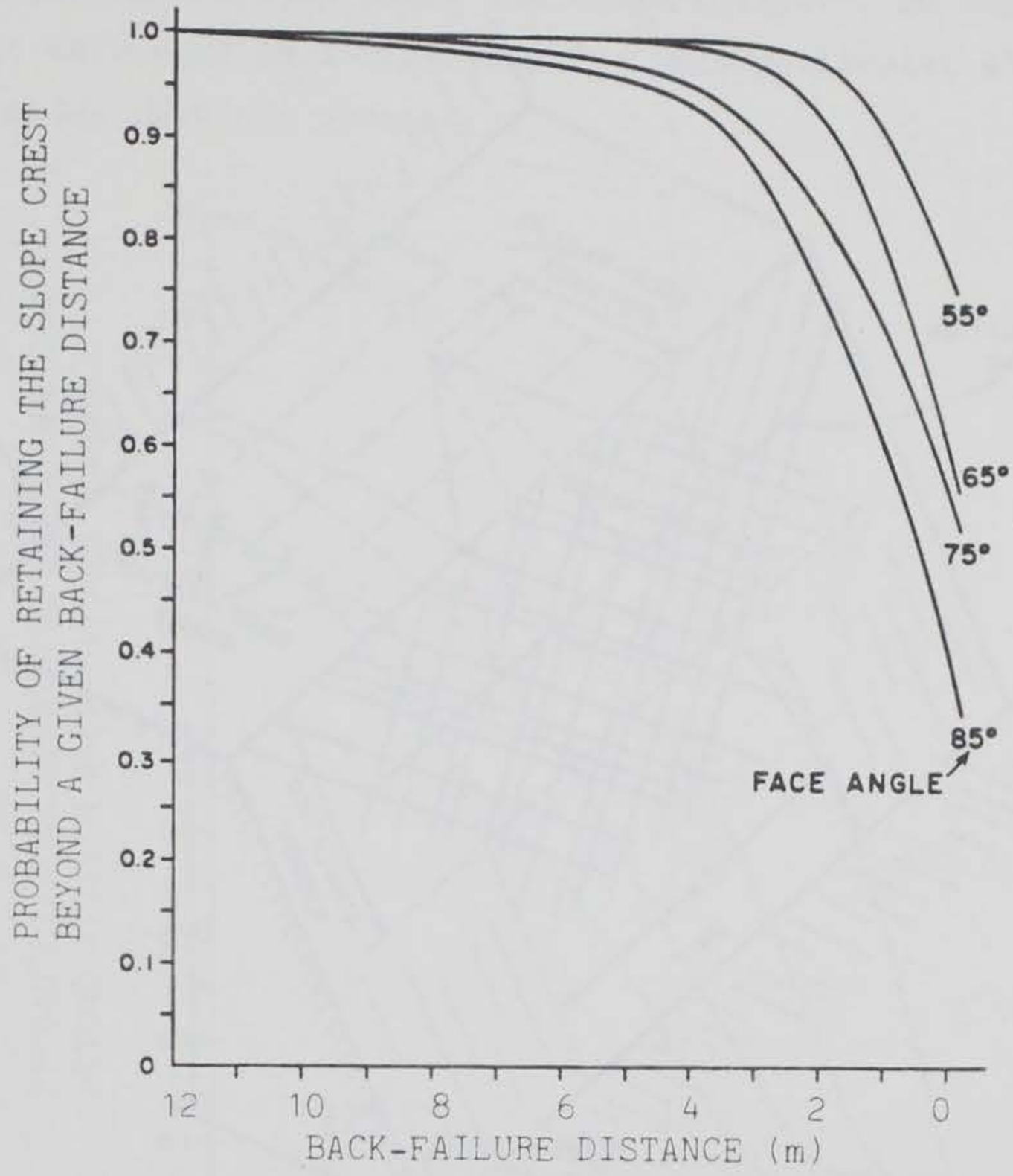

Figure 24. Example slope stability graph for plane-shear failure mode (slope height is 15 m)

139. The three-dimensional character of wedge-failure modes requires that a standard length along the slope face be specified to define an area of probability accumulations. An arbitrary, but rational, decision is to set this length equal to the anticipated slope height, forming square "units" that can be analyzed along the slope face. Figure 25 illustrates the concept of slope units and back-failure cells for analyzing wedges in a rock slope.

140. Properties of the two fracture sets (spacing, dip direction, and dip) that comprise potential wedges are simulated along one or more simulation lines in a given slope face unit. The probability of stability is computed for each kinematically viable wedge formed by the intersection of any two fractures, one from each set. The probability of sufficient length, P_{L_j}, for the j^{th} wedge is the joint probability that both fractures comprising the wedge have sufficient length to allow failure. Probabilities of stability are then calculated and the slope simulation repeated. After several

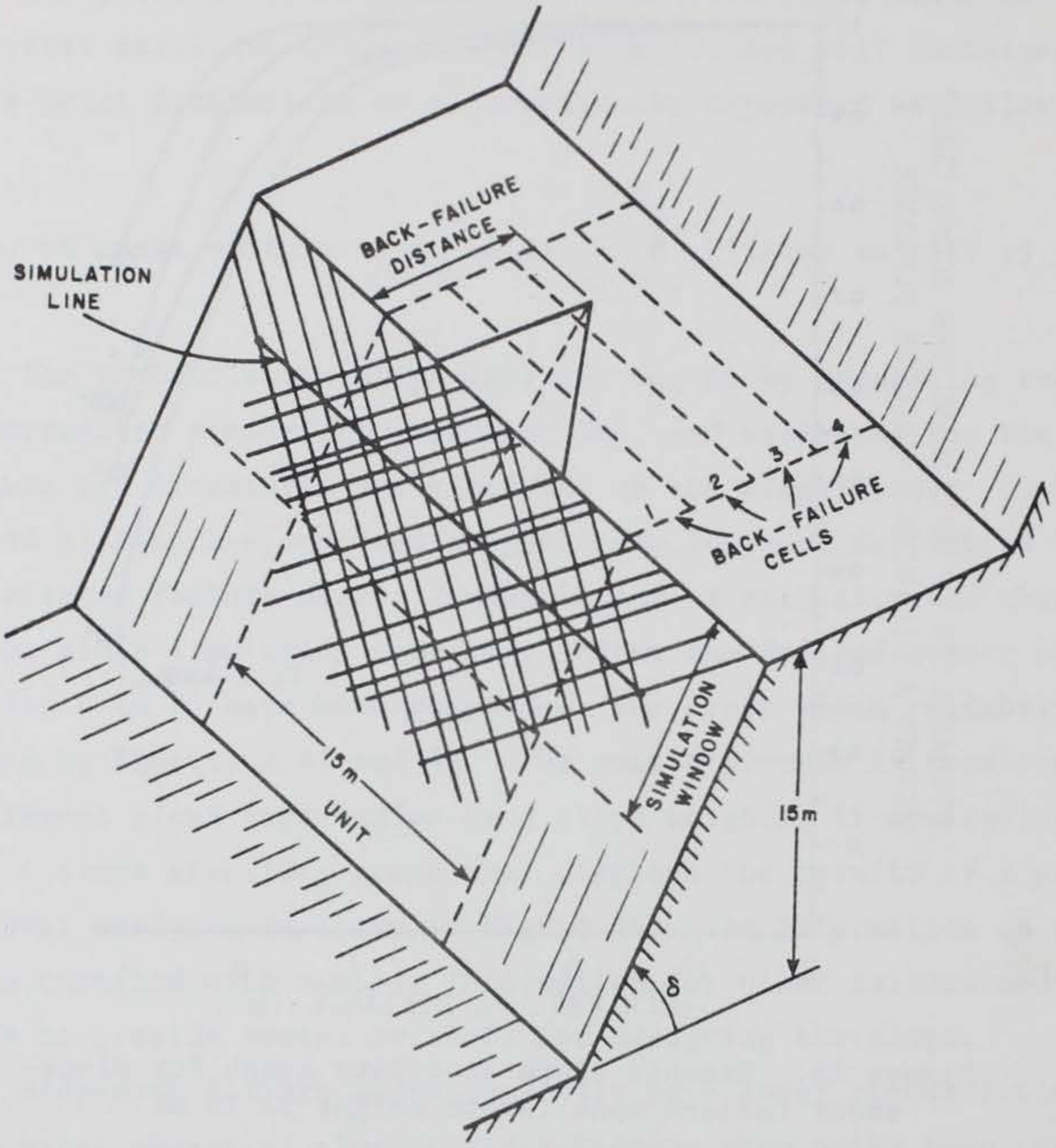

Figure 25. Multiple simulated wedge intersections and back-failure cells in a slope unit (Miller 1982c)

simulations are completed, the crest width reliabilities can be calculated by Equations 41 and 43, with j being a counter for wedges instead of plane-shear fractures. After analyzing slopes with various face angles, a stability graph for wedges can be produced similar to that shown in Figure 24.

141. The probabilistic results shown on the stability graphs for the different types of failure modes present in the slope are combined to produce a complete overall stability graph for the slope being studied. The probability of retaining a specified crest width (crest beyond a given back-failure distance) is the joint probability that the width will be retained for all failure modes present. Thus, the probability values from graphs for the different failure modes are multiplied together to produce the probability values for the overall stability graph. An example of such a graph, which includes

results from plane-shear, step-path, and wedge analyses, is shown in Figure 26. The predominant influence on instability for this particular slope is due to the step-path modes that are present.

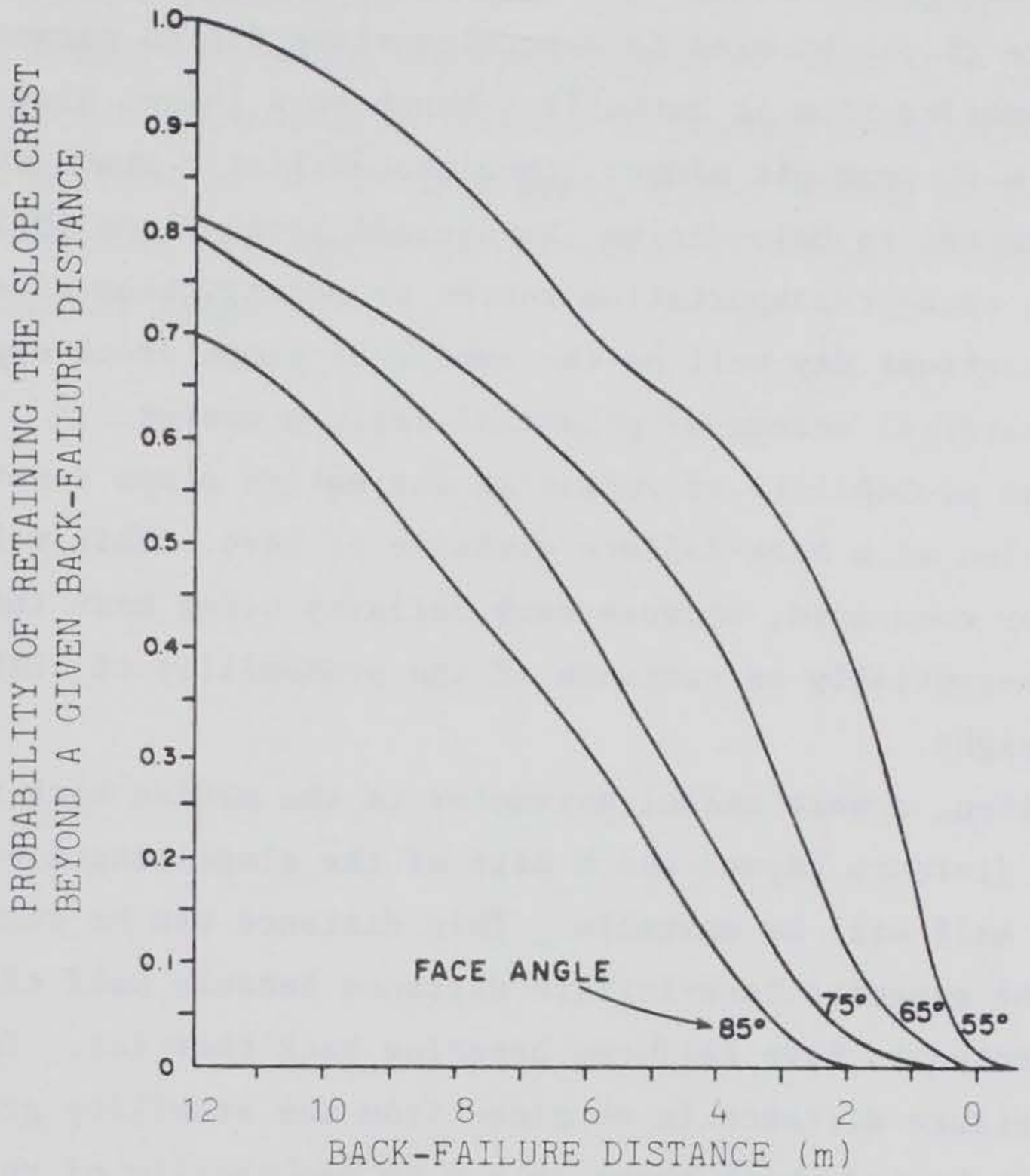

Figure 26. Example slope stability graph for combined results of plane-shear, step-path, and wedge analyses (from Miller 1982c) (Slope height is 15 m)

Useful Design Criteria

142. A physical interpretation of the probability of retaining the slope crest beyond a specified back-failure distance can be illustrated by the following example. Consider a 0.60 probability of retaining the slope crest beyond a back-failure distance of 8 m. This inplies that 60 percent of the length (or of the square slope units if wedge failure modes are present) along the slope strike is expected to have a stable slope crest after 8 m from the original crest has been lost to failures. The remaining 40 percent of the

slope length is expected to have an unstable slope crest beyond the 8-m back-failure distance. That is, 40 percent of the slope length will have failures that break back farther than 8 m.

143. Probability information from a slope stability graph like that shown in Figure 26 can be used to determine slope design parameters. If the slope under consideration is actually a bench on a large, high slope (such as that found in most open pit mines), then probabilistic bench stability parameters are determined to help design the overall large slope (Miller 1982c). For slopes cut along transportation routes or construction sites the important design considerations may well be the amount of slope crest expected to be lost and the material volume of potential failure masses.

144. The probability of retaining the entire slope crest equals the probability value at a back-failure distance of zero. This value is usually quite small, or even zero, because many failures occur near the crest edge. The value is essentially an estimate of the probability of stability for the total slope height.

145. Often, a more useful parameter is the median back-failure distance, or the distance beyond which half of the slope length will be stable and the other half will be unstable. This distance can be considered the best estimate of the expected back-failure distance because half of the slope length is expected to have failures breaking back that far. The predicted median back-failure distance is obtained from the stability graph and is equal to the distance beyond which there is a 0.50 probability of retaining the slope crest.

146. The probability of having a certain volume of failure material can also be estimated from a slope stability graph that incorporates back-failure distances. The most direct estimation procedure involves determining the expected relationship between failure volume and back-failure distance. For plane-shear modes the failure volume (per unit slope length) associated with a given back-failure distance can be calculated using that distance along with the slope angle and the mean dip of the plane-shear fracture set. The same is true for step-path modes except the mean step-path angle is used instead of the mean dip. The failure volumes of wedges can be roughly estimated in the same way using the mean plunge of intersections, or it can be more precisely determined by averaging the volumes of simulated wedges that break back to a given back-failure distance. Failure volumes in a slope will be controlled

predominantly by the failure mode having the longest sliding surfaces, which usually will be the step path if it is present.

147. These types of stability are useful for designing rock slopes that contain many potential sliding surfaces. They serve as the primary design criteria unless large, definable structures such as faults, contacts, or major joints form potential slope failure modes. Estimated probabilities of sliding for these major failure modes (if they are present) should be included in the design process and will even serve as the critical design criteria if their values are reasonably large.

PART VII: SUMMARY EVALUATION OF PROBABILISTIC SLOPE DESIGN

148. Although the probabilistic design of rock slopes is a relatively new area of research and development, its usefulness and importance has been demonstrated in practical engineering studies for open pit mines. Probabilistic slope stability information is often desired because it is essential for mining cost-benefit analyses used to select economically optimum slope angles.

149. Probabilistic slope engineering can also be applied to civil works projects such as road/railway cuts, spillway cuts, and abutment excavations to quantify variables and uncertainties and to evaluate instability risks. Such "risks" can be presented in a probabilistic slope stability graph that yields design criteria which contain and provide more information about the stability conditions of a slope than deterministically calculated safety factors.

Data Requirements for Probabilistic Analysis

150. The engineering design of rock slopes requires information about the geometric properties and shear strengths of geologic structures because slope failures commonly occur along structural discontinuities. Necessary fracture data used to estimate geometric properties of fracture sets can be collected by surface mapping techniques or by oriented-core logging. Mapped fracture orientations obtained from various sites in the project area can be displayed on lower-hemisphere Schmidt plots and used to help delineate structural domains. As mentioned in Part II, at least one or two mapping sites are desired within each anticipated domain as identified from geologic information available prior to fracture mapping. Four or five sites per domain may be needed if fracturing is complex. Fracture data for geometric properties, such as dip, dip direction, spacing, length, and waviness, can then be combined for each fracture set within each domain.

151. Those fracture sets critical to the slope design (those that form potential failure modes) are identified by considering how the set orientations in a given domain interact with the proposed slope orientation. Statistical distributions of geometric properties of the critical sets can then be estimated from the combined fracture data. Spatial correlations can also be estimated by calculating a variogram for each property in a given set. Probabilistic slope stability analyses require such estimations, and to make

them it is usually desirable for the set to contain at least 25 to 30 fracture observations that were obtained from the same mapping site. This suggests that fracture mapping and data evaluation ideally should be interactive to help ensure a sufficient but economical sample of fracture properties.

152. Predictions of the shear strengths along potential failure surfaces are commonly based on the results of laboratory direct shear tests of natural discontinuities contained in rock specimens collected at the site. At least four (preferably six) tests should be conducted for each rock type or fracture identified in the study area. Additional specimens may be desired if the fracture type is especially variable or if the benefits of a better strength estimate warrant the additional time and expense. Results from the tests can be analyzed using statistical regression procedures to combine results for similar specimens and provide a statistical estimate of shear strength for each distinctive rock type or fracture type.

153. Laboratory tests of rock samples are also used to measure the unit weight (density) of each rock type in the study area. Again, approximately six samples of each rock type are considered minimal for estimating the statistical properties of rock density. This parameter is usually found to be normally distributed.

154. Ground water in a rock slope induces pore pressures on potential sliding surfaces. In most cases the pore pressure is directly related to the piezometric surface in the slope, and thus, the water levels in open drill holes should be monitored. Rock mass permeabilities may also be needed for predicting the drawdown curve to the slope face. They can be estimated by field tests, such as pump tests and head tests.

155. Procedures for converting this hydrologic information to a probability distribution of pore pressures are limited at the current time. Monte Carlo simulation can provide a set of possible drawdown curves based on data histograms of water levels, permeability, and porosity (Miller 1982a). When data are limited, engineering judgment can guide in the prediction of mean values, and by assuming a normal distribution, standard deviations can also be estimated by selecting a range about the mean in which over 99 percent of possible values would occur (the difference between the mean and one end of this range equals three standard deviations).

Example Comparison between Probabilistic and Deterministic Results

156. To illustrate some of the advantages of probabilistic methods over deterministic methods an example is presented where the stability of a potential plane shear failure mass is evaluated both ways. The sliding surface (with a dip of 35 deg) is assumed to be continuous so that the probability of sufficient length equals 1. Consequently, the probability of failure is the same as the probability of sliding. The slope is dry with a face angle of 65 deg, and the failure mass is 15 m high.

157. Results of a probabilistic stability analysis are shown in Figure 21. The calculated probability of failure is 0.328 with the safety factor, a random variable, having a mean of 1.185. The probability density function of the safety factor indicates that possible values could easily range from 0.5 to 2.0.

158. A deterministic stability analysis for the same potential failure mass and conditions can be used to calculate a safety factor using the following parameter means:

rock density, $\gamma = 2.70$ t/m^3

waviness, $R = 3.6$ deg

shear strength, $\tau = 0.88387\sigma^{0.93424} + 0.00$

The following values are obtained during the calculation process:

length of sliding surface, $L = 26.15$ m

weight of sliding mass, $W = 229.17$ t

normal stress on sliding surface, $\sigma = 7.179$ t/m^2

shear strength of sliding surface, $\tau = 5.574$ t/m^2

The resulting value of the calculated safety factor is 1.199. It does not include or reflect variabilities in parameter values and it does not indicate how much the safety factor could vary.

159. Typically, a safety of 1.2 to 1.5 is used for design purposes for open pit mine slopes (Hoek and Bray 1977). If such were the case for the above example, the slope very well could be considered safe when, in fact, it

has an estimated probability of failure nearly equal to 0.33. This comparison helps to illustrate the importance of including parameter variabilities when estimating or predicting slope stability.

Conclusions

160. In addition to including parameter variabilities, a probabilistic slope analysis also provides a way to include the effects of multiple occurrences of the same failure mode, which are predicted by simulating spatially correlated properties of the fracture set or sets responsible for that particular failure mode. Different failure modes in the same slope can also be analyzed and the results combined into a probabilistic estimate of overall slope stability. This estimate, as displayed in a probabilistic slope stability graph, provides guidelines and design criteria that often prove more useful than a deterministically calculated safety factor. For instance, probabilistic estimates can be made of the amount of slope crest expected to be lost (by failures) and, thus, of the volumes of potential failure masses.

161. The purpose of a probabilistic analysis of rock slope stability is to provide an estimate of slope stability based on a realistic treatment and incorporation of natural variabilities, measurement uncertainties, and multiple potential failure paths. If slope stability is anticipated to be critically dependent on one or several large definable structures, then the effects of numerous smaller structures are greatly minimized and the design process is simplified. In such a case, the probability (probabilities) of stability of the major failure mode(s) will be the principal factor in designing the slope. The probability value acceptable for design will vary from project to project depending on the "cost" of a slope failure (in terms of dollars, time, loss of life or property, sociological impacts, or other intangibles). Appropriate procedures should be developed for assigning values to slope failure "costs" and subsequently setting acceptable design criteria for probabilities of stability. Thus, additional research and field verification are required for evaluating the effectiveness of probabilistic slope engineering methods and for building a design rationale around them.

REFERENCES

Baecher, G. B. 1980. "Progressively Censored Sampling of Rock Joint Traces," Mathematical Geology, Vol 12, pp 33-40.

Baecher, G. B. et al. 1978. "Risk Analysis for Rock Slopes in Open Pit Mines," Annual Technical Report to U. S. Bureau of Mines, Vol 1.

Borgman, L. E. 1973a. "Spectrum Analysis of Random Data Including Procedures Based on the Fast Fourier Transform Algorithm," Publication No. STL-2008, Department of Statistics, University of Wyoming, Laramie.

_____. 1973b. "Statistical Properties of Fast Fourier Transform Coefficients Computed from Real-Valued, Covariance-Stationary, Periodic Random Sequences," Research Paper No. 23, Department of Statistics, University of Wyoming, Laramie.

_____. 1977. "Some New Techniques for Hurricane Risk Analysis," in Proceedings of 9th Annual Offshore Technical Conference, Houston, OTC-2848, pp 331-338.

_____. 1982. "Techniques for Computer Simulation of Ocean Waves," in Topics in Ocean Physics, from LXXX Corso, Soc. Italiana di Fisica, Bologna, Italy, pp 387-417.

Bridges, M. C. 1976. "Presentation of Fracture Data for Rock Mechanics," in Proceedings of 2nd Australian-New Zealand Conference on Geomechanics, Brisbane, pp 144-148.

Brown, A. 1982. "Toppling Induced Movements in Large, Relatively Flat Rock Slopes," in Proceedings of 23rd U. S. Symposium on Rock Mechanics, American Institute of Mining, Metallurgical, and Petroleum Engineers, New York, pp 1035-1047.

Call, R. D. 1972. "Analysis of Geologic Structure for Open Pit Slope Design," Ph.D. dissertation, University of Arizona, Tucson.

Call, R. D. and Nicholas, D. E. 1978. "Prediction of Step Path Failure Geometry for Slope Stability Analysis," paper presented at 19th U. S. Symposium on Rock Mechanics, Lake Tahoe, Nev.

Call, R. D., Savely, J. P., and Nicholas, D. E. 1976. "Estimation of Joint Set Characteristics from Surface Mapping Data," in Proceedings of 17th U. S. Symposium on Rock Mechanics, Salt Lake City, Utah, pp 2B2.1-2B2.9.

Call, R. D., Savely, J. P., and Pakalnis, R. 1982. "A Simple Core Orientation Technique," in Proceedings of 3rd International Conference on Stability in Surface Mining, Society of Mining Engineers, American Institute of Mining, Metallurgical, and Petroleum Engineers, New York, pp 465-480.

Cruden, D. M. 1977. "Describing the Size of Discontinuities," International Journal of Rock Mechanics and Mining Science, Vol 14, pp 133-137.

Deere, D. U. 1968. "Geological Considerations," in Rock Mechanics and Engineering Practice, Stagg, K. G., and Zienkiewicz, O. C., Eds., John Wiley & Sons, London, pp 1-20.

Draper, N. R. and Smith, H. 1981. Applied Regression Analysis, 2nd ed., John Wiley & Sons, New York.

Feller, W. 1966. An Introduction to Probability Theory and Its Applications, Vol. II, John Wiley & Sons, New York.

Goodman, R. E. 1980. Introduction to Rock Mechanics, John Wiley & Sons, New York.

Goodman, R. E. and Taylor, R. L. 1967. "Methods of Analysis for Rock Slopes and Abutments," Proceedings of 8th U. S. Symposium on Rock Mechanics, Minneapolis, Minn., pp 303-320.

Hoeg, K. and Murarka, R. P. 1974. "Probabilistic Analysis and Design of a Retaining Wall," Journal of the Geotechnical Division, American Society of Civil Engineers, GT3, pp 349-366.

Hoek, E. and Bray, J. W. 1977. Rock Slope Engineering, 2nd Ed., Institute of Mining and Metallurgy, London.

International Society for Rock Mechanics. 1974. "Suggested Methods for Determining Shear Strength," ISRM Commission on Standardization of Laboratory and Field Tests.

_____. 1977. "Suggested Methods for the Quantitative Description of Discontinuities in Rock Masses," International Journal of Rock Mechanics, Mining Science, and Geomechanics Abstracts, Vol 15, pp 319-368.

Jaeger, J. C. 1971. "Friction of Rocks and Stability of Rock Slopes," Geotechnique, Vol 21, No. 2, pp 97-134.

Jenkins, G. M. and Watts, D. G. 1968. Spectral Analysis and Its Applications, Holden-Day, San Francisco, Calif.

Journel, A. G. 1974. "Geostatistics for Conditional Simulation of Ore Bodies," Economic Geology, Vol 69, pp 673-687.

Kim, Y. C. and Wolff, S. F. 1978. "Optimization of Coal Recovery from Open Pits (Revised)," report prepared for Canada Centre for Mineral and Energy Technology.

La Pointe, P. R. 1980. "Analysis of the Spatial Variation in Rock Mass Properties through Geostatistics," in Proceedings of 21st U. S. Symposium on Rock Mechanics, University of Missouri-Rolla, pp 570-580.

Laslett, G. M. 1982. "Censoring and Edge Effects in Areal and Line Transect Sampling of Rock Joint Traces," Mathematical Geology, Vol 14, pp 125-140.

Mahtab, M. A. and Yegulalp, T. M. 1982. "A Rejection Criterion for Definition of Clusters in Orientation Data," Proceedings of 23rd U. S. Symposium on Rock Mechanics, American Institute of Mining, Metallurigical, and Petroleum Engineers, New York, pp 116-123.

Marek, J. M. and Savely, J. P. 1978. "Probabilistic Analysis of the Plane Shear Failure Mode," Proceedings of 19th U. S. Symposium on Rock Mechanics, Vol II, Mackay School of Mines, University of Nevada-Reno, pp 40-44.

Matheron, G. 1963. "Principles of Geostatistics," Economic Geology, Vol 58, pp 1246-1266.

McMahon, B. K. 1974. "Design of Rock Slopes against Sliding on Pre-existing Fractures," Proceedings of 3rd International Symposium on Rock Mechanics, Denver, Colo., Vol II-B, pp 803-808.

Miller, S. M. 1979. "Geostatistical Analysis for Evaluating Spatial Dependence in Fracture Set Characteristics," Proceedings of 16th International Symposium on the Applications of Computers and Operation Research in the Mineral Industry, Society of Mining Engineers, American Institute of Mining, Metallurgical, and Petroleum Engineers, New York, pp 537-545.

_____. 1982a. "Analytical Estimation of Parabolic Water Table Drawdown to a Slope Face," Proceedings of 3rd International Conference on Stability in Surface Mining, Society of Mining Engineers, American Institute of Mining, Metallurgical, and Petroleum Engineers, New York, pp 417-435.

_____. 1982b. "Fourier Analysis for Estimating Probability of Sliding for the Plane Shear Failure Mode," Proceedings of 23rd U. S. Symposium on Rock Mechanics, American Institute of Mining, Metallurgical, and Petroleum Engineers, New York, pp 124-131.

_____. 1982c. "Statistical and Fourier Methods for Probabilistic Design of Rock Slopes," Ph.D. dissertation, University of Wyoming, Laramie.

_____. 1983. "A Statistical Method to Evaluate Homogeneity of Structural Populations," Mathematical Geology, Vol 15, pp 317-328.

Newendor P. D. 1975. Decision Analysis for Petroleum Exploration, The Petroleum Publishing Co., Tulsa, Okla.

Piteau, D. R. 1970. "Engineering Geology Contribution to the Study of Slopes in Rock with Particular Reference to DeBeers Mine," Ph.D. thesis, University of the Witwatersrand, Johannesburg, 2 vols.

Robertson, A. M. 1970. "The Interpretation of Geologic Factors for Use in Slope Stability," Proceedings of Symposium on the Theoretical Background to the Planning of Open Pit Mines with Special Reference to Slope Stability, Johannesburg, pp 55-71.

Shanley, R. J. and Mahtab, M. A. 1976. "Delineation and Analysis of Clusters in Orientation Data," Mathematical Geology, Vol 8, pp 9-23.

Taheri, S. M. 1980. "Data Retrieval and Multidimensional Simulation of Mineral Resources," Ph.D. dissertation, University of Wyoming, Laramie.

Terzaghi, R. D. 1965. "Sources of Error in Joint Surveys," Geotechnique, Vol 15, No. 3, pp 287-304.

U. S. Army Engineer Waterways Experiment Station. 1980. Rock Testing Handbook, Test Standards - 1980, Vicksburg, Miss.

Whitten, E. H. T. 1966. Structural Geology of Folded Rocks, Rand McNally and Co., Chicago.

Wittke, W. W. 1965. "Method to Analyze the Stability of Rock Slopes with and without Additional Loading (in German)," Rock Mechanics and Engineering Geology, Suppl. II, Vol 30, pp 52-79; English translation in Rock Mechanics Report No. 6, July 1971, Imperial College, London.

Zelen, M. and Severo, N. C. 1965. "Probability Functions," Handbook of Mathematical Functions, Dover Publications, Inc., New York, pp 925-995.

APPENDIX A: SOURCES OF COMPUTER SOFTWARE

1. Some sources for computer software applicable to probabilistic data analyses and stability analyses for rock slope engineering are listed below. The list should be considered <u>incomplete</u> and some materials may be proprietary.

Appendices A-D given in
Miller (1982c)

Call & Nicholas, Inc.
6420 E. Broadway, Suite A100
Tucson, AZ 85710
attn: R. D. Call

Dept. of Civil Engineering
Massachusetts Institute of
Technology
Cambridge, MA 02139
attn: G. B. Baecher

GEOMIN Computer Services
708 Kapilano 100
West Vancouver, B. C. V7T 1A2
(also, Piteau & Associates,
same address)

Golder Associates
10628 N.E. 38th Place
Kirkland, WA 98033
attn: D. Pentz

Pincock, Allen, and Holt, Inc.
1750 E. Benson Highway
Tucson, AZ 84714
attn: J. M. Marek

Steffen Robertson and Kirsten
1281 W. Georgia St., Suite 500
Vancouver, B. C. V6E 3J7
attn: A. M. Robertson